1′-Acetoxychavicol Acetate Is a Novel Nuclear Factor κB Inhibitor with Significant Activity against Multiple Myeloma *In vitro* and *In vivo*

Keisuke Ito,[1] Tomonori Nakazato,[1] Ming Ji Xian,[1] Taketo Yamada,[2] Nobumichi Hozumi,[3] Akira Murakami,[4] Hajime Ohigashi,[4] Yasuo Ikeda,[1] and Masahiro Kizaki[1]

[1]Division of Hematology, Department of Internal Medicine and [2]Pathology, Keio University School of Medicine, Tokyo, Japan; [3]Institute of Biological Science, Science University of Tokyo, Chiba, Japan; and [4]Division of Food Science and Biotechnology, Graduate School of Agriculture, Kyoto University, Kyoto, Japan

Abstract

1′-Acetoxychavicol acetate (ACA) is a component of a traditional Asian condiment obtained from the rhizomes of the commonly used ethno-medicinal plant *Languas galanga*. Here, we show for the first time that ACA dramatically inhibits the cellular growth of human myeloma cells via the inhibition of nuclear factor κB (NF-κB) activity. In myeloma cells, cultivation with ACA induced G_0-G_1 phase cell cycle arrest, followed by apoptosis. Treatment with ACA induced caspase 3, 9, and 8 activities, suggesting that ACA-induced apoptosis in myeloma cells mediates both mitochondrial- and Fas-dependent pathways. Furthermore, we showed that ACA significantly inhibits the serine phosphorylation and degradation of IκBα. ACA rapidly decreased the nuclear expression of NF-κB, but increased the accumulation of cytosol NF-κB in RPMI8226 cells, indicating that ACA inhibits the translocation of NF-κB from the cytosol to the nucleus. To evaluate the effects of ACA *in vivo*, RPMI8226-transplanted NOD/SCID mice were treated with ACA. Tumor weight significantly decreased in the ACA-treated mice compared with the control mice. In conclusion, ACA has an inhibitory effect on NF-κB, and induces the apoptosis of myeloma cells *in vitro* and *in vivo*. ACA, therefore, provides a new biologically based therapy for the treatment of multiple myeloma patients as a novel NF-κB inhibitor. (Cancer Res 2005; 65(10): 4417-24)

Introduction

1′-Acetoxychavicol acetate (ACA) is obtained from the rhizomes of *Languas galanga* (Zingiberaceae), a traditional condiment in Thailand (1). Recent studies have revealed that ACA has potent chemopreventive effects against rat oral carcinomas and inhibits the chemically induced tumor formation and cellular growth of various cancer cells (2–5). More recently, we reported that ACA induces the apoptosis of myeloid leukemia cells *in vitro* and *in vivo*, suggesting that ACA has potential as a novel therapeutic agent for the treatment of myeloid leukemia (6). We found that the ACA-induced apoptosis in myeloid leukemic cells was associated with the production of intracellular reactive oxygen species (ROS; ref. 6); however, the exact biological and molecular mechanisms of ACA-induced apoptosis in various cancer cells are still unclear.

Multiple myeloma is a plasma cell malignancy that remains incurable despite the use of conventional and high-dose chemotherapy with hematopoietic stem cell transplantation; therefore, novel therapeutic approaches are urgently needed in clinical settings (7). The understanding that has recently been gained into the biology of myeloma has led to the development of biological treatments, such as thalidomide and bortezomib, which target the myeloma cell and the bone marrow microenvironment. These agents have shown remarkable activity against refractory multiple myeloma in early clinical trials, but prolonged drug exposure may result in the development of *de novo* drug resistance in some cases (7–9). Therefore, the identification and validation of additional novel targeted therapies to overcome drug resistance and improve patient outcome are needed.

Nuclear factor κB (NF-κB), which was originally identified as a B-cell nuclear factor, is required for the proper regulation of B-cell homeostasis (10, 11). NF-κB is a member of the Rel family of proteins, and is typically a heterodimer composed of p50, p65, and IκBα subunits. NF-κB is constitutively present in the cytosol and is inactivated by its interaction with IκB family inhibitors. On activation, IκBα undergoes phosphorylation and ubiquitination-dependent degradation by the 26S proteosome, leading to translocation of NF-κB into the nucleus and binding to the specific DNA sequences in the promoter of the target genes, which stimulates their transcription (12–14). The protein products of these genes, including a variety of cytokines, cell adhesion molecules, and chemokines, mediate the regulation of cellular growth in many cells. Recently, it has been reported that NF-κB is constitutively active in myeloma cells, which contributes to the survival of these cells (15, 16). In addition, it has been reported that myeloma cell adhesion to bone marrow stromal cells induces NF-κB–dependent up-regulation of the transcription of IL-6, a major growth factor of myeloma cells (17). Tumor necrosis factor (TNF)-α is secreted into the bone marrow microenvironment and induces NF-κB–dependent alteration in adhesion molecule expression in both myeloma cells and bone marrow stromal cells, with resulting increased cell adhesion. This confers resistance to myeloma cell apoptosis and also triggers the NF-κB–dependent secretion of IL-6. These results indicate that NF-κB is the most important therapeutic target for the treatment of multiple myeloma. Conventional and recent antimyeloma agents, including dexamethasone, thalidomide, proteasome inhibitor PS-341, and arsenic trioxide, inhibit

Requests for reprints: Masahiro Kizaki, Division of Hematology, Department of Internal Medicine, Keio University School of Medicine, 35 Shinanomachi, Shinjuku-ku, Tokyo 160-8582, Japan. Phone: 81-3-5363-3785; Fax: 81-3-3353-3515; E-mail: makizaki@sc.itc.keio.ac.jp.

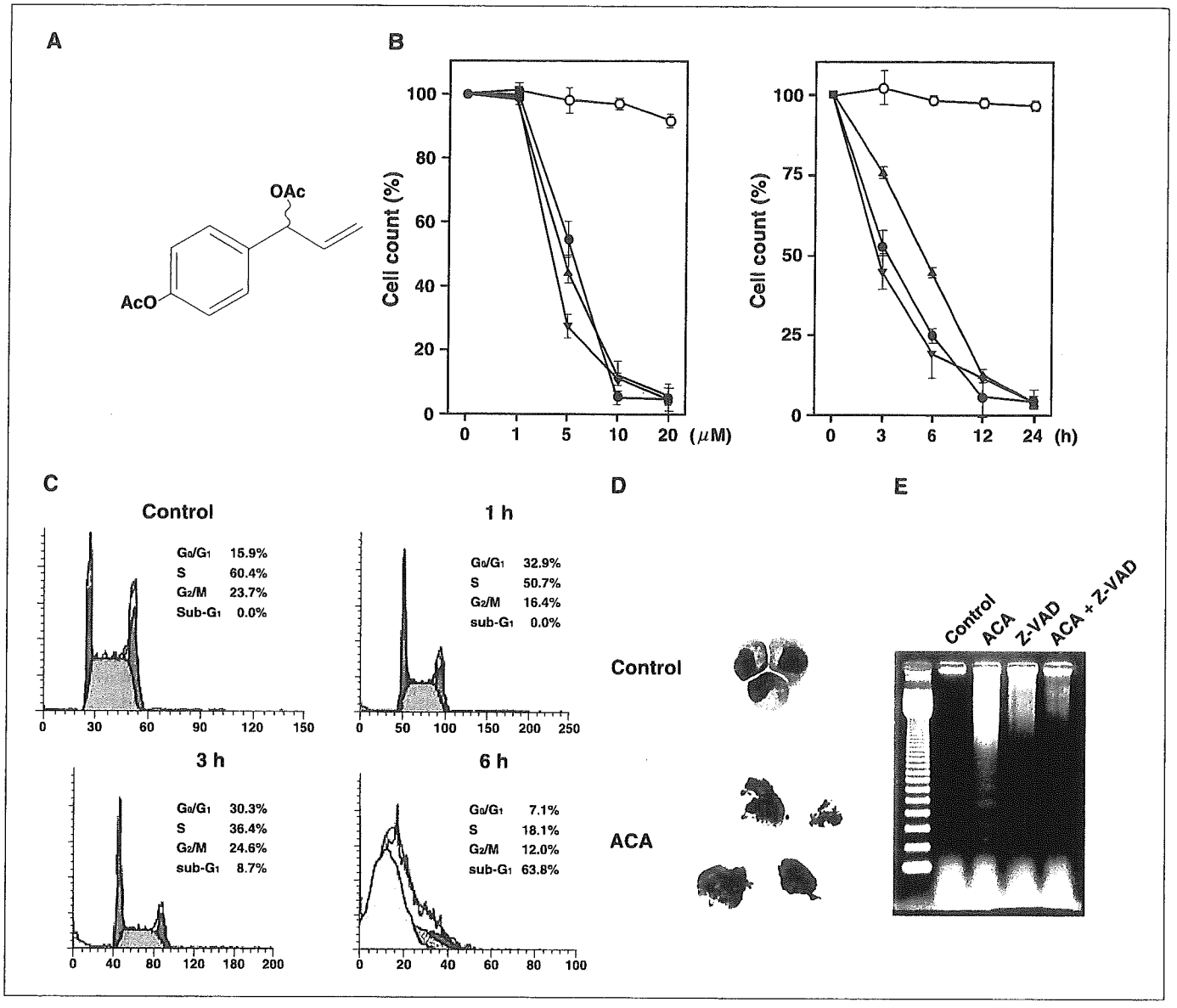

Figure 1. Chemical structure of ACA and induction of G_0-G_1 cell cycle arrest followed by apoptosis in various myeloma cells. *A*, chemical structure of (1′*R*, *S*′)-ACA. *B* and *C*, various myeloma cell lines [RPMI8226 (●), U266 (▲), IM-9 (▼) and bone marrow mononuclear cells from a healthy donor (○)] were treated with various concentrations (0-20 μmol/L) of ACA for 24 hours (*B*, *left*) and with 10 μmol/L ACA for various times (0-24 hours; *B*, *right*). Cell viability was assessed by trypan blue dye exclusion. Results are expressed as the mean ± SD of three different experiments. *C*, cell cycle analysis. RPMI8226 cells were treated with 10 μmol/L ACA for the indicated times, and then stained with PI as described in Materials and Methods. The DNA content was analyzed by means of flow cytometry. G_0-G_1, S, and G_2-M indicate the cell phase, and the sub-G_1 DNA content refers to the portion of apoptotic cells. Each phase was calculated by using a ModiFIT program. Three duplicate experiments were done with similar results, and the representative data are shown. *D*, morphologic changes characteristic of apoptosis in RPMI8226 cells. RPMI8226 cells were treated with 10 μmol/L ACA for 3 hours, and cytospin slides were then prepared and stained with Giemsa. Original magnification, ×1,000. *E*, agarose gel electrophoresis demonstrating DNA fragmentation in RPMI8226 cells treated with 10 μmol/L ACA for 3 hours. Preincubation with 20 μmol/L pan-caspase inhibitor, Z-VAD-FMK, inhibited ACA-induced apoptosis.

NF-κB activation (18–21). However, these agents have a multiple number of other biological effects. Therefore, a more specific NF-κB inhibitor may have clinical benefits and the blockade of its signaling pathway may represent a novel therapeutic strategy for managing multiple myeloma.

Our previous study showed that ACA induces apoptosis through two different pathways in the myeloid leukemia cells: ROS generation and the activation of the Fas-pathway (6). NF-κB is known to contribute to both the caspase 8 and 9 pathways. In this study, we addressed the molecular mechanisms of the antimyeloma action of ACA, and, quite surprisingly, we found that ACA inhibited the cellular growth of myeloma cells in association with the down-regulation of NF-κB activity. We further investigated the molecular mechanism of ACA and the possibility of clinically applying it by using *in vivo* mice model.

Materials and Methods

Cell cultures. Various human multiple myeloma cell lines, including RPMI8226, U266, and IM-9, were obtained from the Japan Cancer Research Resources Bank (Tokyo, Japan), and were maintained in RPMI 1640 (GIBCO-BRL, Grand Island, NY) with 10% fetal bovine serum (GIBCO-BRL),

100 units/mL penicillin, and 100 mg/mL streptomycin in a humidified atmosphere with 5% CO_2. Bone marrow samples from patients with multiple myeloma and healthy donors were obtained according to appropriate Human Protection Committee validation at Keio University School of Medicine (Tokyo, Japan), and with written informed consent. The patients' samples were grown in RPMI 1640 with 15% FBS (Hyclone Laboratories, Logan, MT) under standard culture conditions.

Reagents. ACA (99% purity) was synthesized as previously reported (Fig. 1*A*; ref. 1). Synthetic (1′*R*, 5′)-ACA has an identical suppressive activity to natural (1′*S*)-ACA, as evaluated by tumor promoter–induced EBV activity (22). ACA was dissolved in DMSO at a stock concentration of 20 mmol/L. Various caspase inhibitors, including Z-VAD-FMK (a pan-caspase inhibitor), DEVD-FMK (a caspase 3 inhibitor), Z-IETD-FMK (a caspase 8 inhibitor), and LEHD-FMK (a caspase 9 inhibitor), were purchased from Calbiochem (La Jolla, CA). TNF-α was purchased from Sigma Chemical (St. Louis, MO). Phorbol 12-myristate 13-acetate (PMA: synthetic analogue of diacylglycerol) was dissolved in DMSO. The final DMSO concentrations in the medium were not greater than 0.1%. *N*-Tosyl-L-lysine chloromethyl ketone (TLCK), a serine protease inhibitor, was obtained from Roche (Indianapolis, IN). MG132 (z-Leu-Leu-Leu-aldehyde), a proteasome inhibitor, was purchased from BIOMOL Research Laboratories, Inc. (Plymouth Meeting, PA). For the Fas inhibition assay, antagonistic anti-ZB4 monoclonal antibody was purchased from MBL (Nagoya, Aichi, Japan).

Assays for apoptosis. Apoptosis was determined based on morphologic changes. Apoptotic cells were quantified by annexin V-FITC and propidium iodide (PI) double staining using a staining kit purchased from PharMingen (San Diego, CA). The induction of apoptosis was also detected by DNA fragmentation assay.

Western blot analysis. The cells were collected by centrifugation at 700 × *g* for 10 minutes, and then the pellets were resuspended in a lysis buffer [1% NP40, 1 mmol/L phenylmethylsulfonyl fluoride, 40 mmol/L Tris-HCl (pH 8.0), 150 mmol/L NaCl] at 4°C for 15 minutes. Mitochondrial and cytosolic fractions were prepared with digitonin-nagarse treatment. Protein concentrations were determined using a protein assay DC system (Bio-Rad, Richmond, CA). Cell lysates (15 μg of protein per lane) were fractionated on 12.5% SDS-polyacrylamide gels before being transferred to the membrane (Immobilon-P membranes, Millipore, Bedford, MA) according to standard protocol. Antibody binding was detected by using the enhanced chemiluminescence kit with hyper-ECL film (Amersham, Buckinghamshire, United Kingdom). The blots were also stained with Coomassie brilliant blue to confirm that equal amounts of protein extract were presented in each lane. The following antibodies were used in this study: anti-Fas (PharMingen); IκBα, pSer32-IκBα (Cell Signaling Technology, Inc., Beverly, MA); intercellular adhesion molecule 1 (ICAM-1), NF-κB, FLICE-inhibitory protein (FLIP), X-linked inhibitor of apoptosis protein (XIAP), apoptosis inducing factor (AIF), caspase inhibitory protein-1 (cIAP), and β-actin (Santa Cruz Biotech, Santa Cruz, CA).

Assays for nuclear factor κB activity. The DNA binding activity of NF-κB in the myeloma cells was quantified by ELISA using the Trans-NF-κB p65 Transcription Factor Assay Kit (Active Motif North America, Carlsbad, CA), according to the instructions of the manufacturer. Briefly, nuclear extracts were prepared and incubated in 96-well plates coated with immobilized oligonucleotide (5′-AGTTGAGGGGACTTTCCCAGGC-3′) containing a consensus (5′-GGGACTTTC-3′) binding site for the p65 subunit of NF-κB. NF-κB binding to the target oligonucleotide was detected by incubation with the primary antibody specific for the activation form of p65 (Active Motif North America), visualized by anti-immunoglobulin G horseradish peroxidase conjugate and Developing Solution, and quantified at 450 nm with a reference wavelength of 655 nm. Background binding, obtained by incubation with a 2-nucleotide mutant oligonucleotide (5′-AGTTGAGGCCACTTTCCCAGGC-3′), was subtracted from the value obtained for binding to the consensus DNA sequence.

Effects of 1′-acetoxychavicol acetate *in vivo*. We have established a human leukemia and multiple myeloma model in an NOD/SCID mouse (23). Briefly, the mice were pretreated with 3 Gy of total body irradiation, which is a sublethal dose that was expected to enhance the acceptance of xenografts. Subsequently, RPMI8226 cells (1×10^7 cells) in their logarithmic growth phase were inoculated s.c. into the NOD/SCID mice (Jackson Laboratory, Bar Harbor, ME). The inoculated RPMI8226 cells formed s.c. tumors at the injection site, and the cells grew rapidly. Seven days after the implantation of the cells, the mice with the transplanted cells were randomly assigned to receive PBS ($n = 10$) or 3 mg/kg ACA ($n = 10$) as an i.p. injection once every 3 days for 2 weeks. After 2 weeks of treatment, the mice were sacrificed and dissected to measure the tumor weights. When the mice showed severe wasting, or when the observations were completed, the mice were sacrificed according to the UKCCCR guidelines, and the day of sacrifice was recorded (24).

Results

Effects of 1′-acetoxychavicol acetate on cellular proliferation of various myeloma cells. We first investigated the effects of ACA on the cellular proliferation of three human multiple myeloma cell lines, including RPMI8226, U266, and IM-9 cells, and fresh samples from patients with multiple myeloma. ACA induced

Table 1. Clinical characteristics and the effects of ACA on the induction of apoptosis and NF-κB activity in eight patients with multiple myeloma

Patient	Age (y)/Sex	Bone marrow plasma cells (%)	Annexin V–positive cells (%)			NF-κB activity (%)
			Control	ACA	Fold increase	
1	73/M	78.6	5.6	93.5	16.7	43.3
2	54/M	75.6	6.8	84.3	12.4	50.5
3	70/M	55.2	4.6	87.6	19.0	46.2
4	58/F	46.4	10.4	75.4	7.3	41.5
5	61/F	78.5	7.4	80.4	10.9	57.4
6	34/F	63.5	8.3	81.1	9.8	60.1
7	46/M	57.6	12.2	92.5	7.6	42.1
8	75/M	48.2	9.3	78.5	8.4	38.5

NOTE: Fresh myeloma cells from patients were separated by Lymphoprep sedimentation procedure and subsequently cultured with 10 μmol/L of ACA. Induction of apoptosis was examined by annexin V–positive cells. The DNA binding activity of NF-κB was quantified by ELISA with the use of the Trans-AM NF-κB p65 Transcriptional Factor Assay Kit, and results were expressed as the percentage of the control cells.

apoptosis of myeloma cell lines, as well as of eight freshly obtained samples from patients with multiple myeloma, but not of normal bone marrow mononuclear cells from a healthy donor, in a dose- and time-dependent manner (Fig. 1*B*; Table 1). Cultivation with ACA rapidly and strongly increased the population of RPMI8226 myeloma cells in the G_0-G_1 phase, and then in the sub-G_1 phase (Fig. 1*C*). Apoptosis was assessed in terms of both the morphologic changes and the DNA ladder formation (Fig. 1*D* and *E*). Consistent with these results, annexin V–positive cells were increased after incubation with ACA for 3 hours, indicating that the onset of apoptosis had already started to occur after only 3 hours of treatment (data not shown). These results indicate that ACA led to cell cycle arrest at the G_0-G_1 phase, followed by apoptosis.

Effects of 1′-acetoxychavicol acetate on caspase activity. Treatment with 10 μmol/L ACA for 3 hours significantly induced caspase 3, 8, and 9 activities in RPMI8226 cells (Fig. 2*A*). RPMI8226 cells were treated with 10 μmol/L ACA for 12 hours, either alone or in combination with Z-VAD-FMK (a pan-caspase inhibitor), DEVD-FMK (a caspase 3 inhibitor), Z-IETD-FMK (a caspase 8 inhibitor), or LEHD-CHO (a caspase 9 inhibitor). ACA-induced apoptosis was almost completely blocked by Z-VAD-FMK and by combination of Z-IETD-FMK and LEHD-FMK, although Z-IETD-FMK or LEHD-FMK alone partially inhibited ACA-induced apoptosis in RPMI8226 cells (Fig. 2*B*). In addition, the preincubation of Z-VAD-FMK inhibited the ACA-induced apoptosis of myeloma cells by means of DNA ladder formation analysis (Fig. 1*E*). These results suggest that through treatment with ACA, both of the cascades to the caspase 8 and caspase 9 pathways are activated.

1′-Acetoxychavicol acetate inhibits IκBα phosphorylation and nuclear factor κB activation in myeloma cells. ACA significantly inhibited the serine phosphorylation and degradation of IκBα in a time-dependent manner (Fig. 2*C*). Because the phosphorylation of IκB has been shown to be the primary

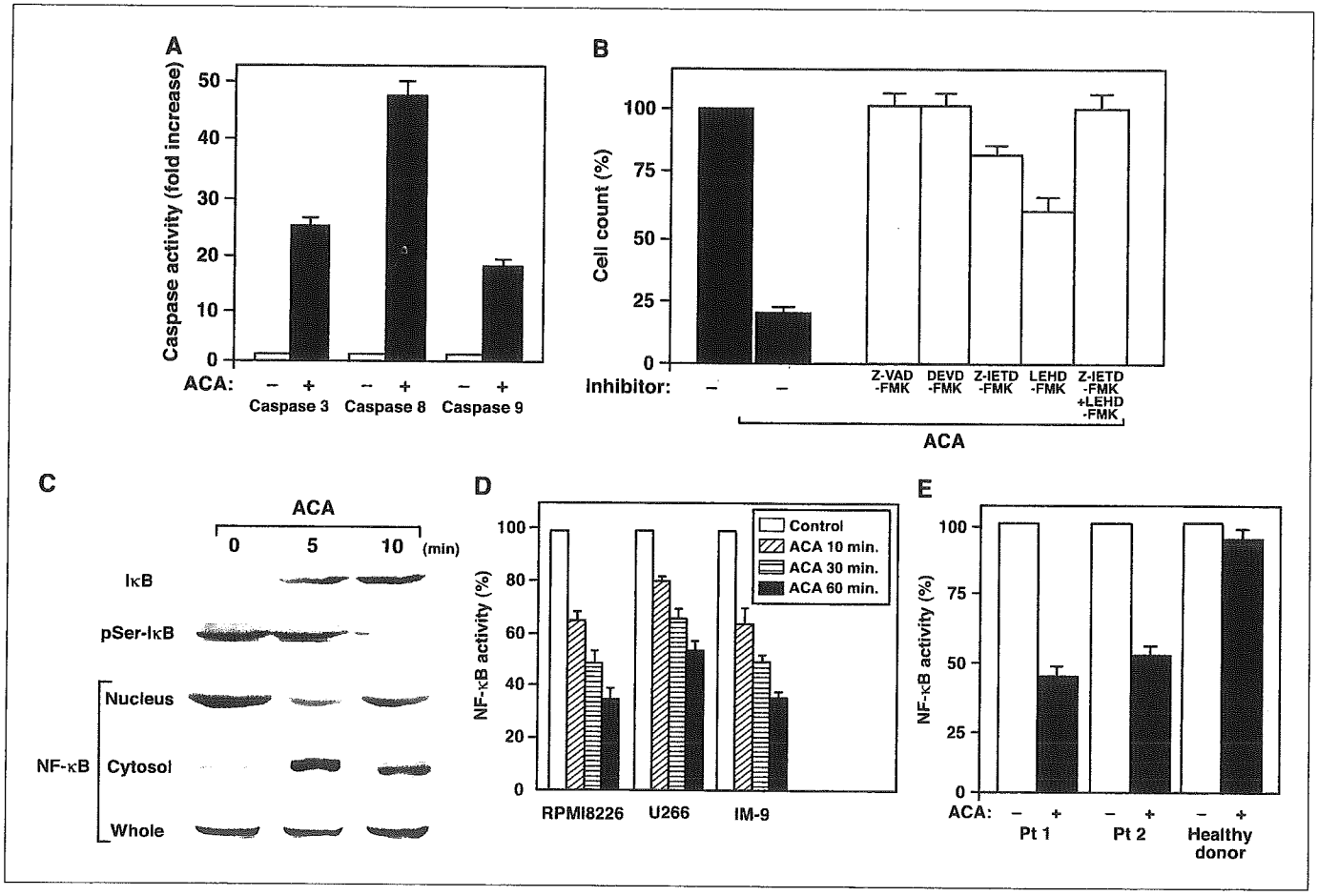

Figure 2. Effects of ACA on caspase and NF-κB activation. *A*, RPMI8226 cells were incubated with 10 μmol/L ACA for 3 hours and then analyzed for activation of caspase 3, 8, and 9 by flow cytometry and colorimetric assay. Each caspase activity in the ACA-treated cells was presented as a fold increase of the control cells. *B*, inhibition of ACA-induced apoptosis in RPMI8226 cells was estimated in a preincubation of Z-VAD-FMK. The cells were preincubated with 20 μmol/L Z-VAD-FMK for 1 hour before the addition of 10 μmol/L ACA. The cell counts were evaluated after 6 hours of incubation. Then, effects of specific caspase inhibitors on ACA-induced apoptosis were examined. The cells were preincubated with each caspase inhibitor [50 μmol/L DEVD-FMK (a caspase 3 inhibitor), 50 μmol/L Z-IETD-FMK (a caspase 8 inhibitor), and 50 μmol/L LEHD-FMK (a caspase 9 inhibitor)] for 1 hour, and then incubated with 10 μmol/L ACA for 6 hours. Cell viability was assessed by trypan blue dye exclusion. *Columns*, mean of three separate experiments done in triplicate; *bars*, SD. *C*, effects of ACA on IκBα phosphorylation and the constitutive expression of NF-κB in myeloma cells. RPMI8226 cells were treated with ACA (10 μmol/L) for the indicated times. Cell lysates (15 μg of protein per lane) were fractionated on 12.5% SDS-polyacrylamide gels and analyzed by Western blotting with antibodies against IκBα and pSer32-IκBα. Nuclear and cytoplasmic extracts and whole cell lysates were prepared to check the level of NF-κB by Western blotting. *D*, ACA down-regulates constitutive NF-κB activity in myeloma cells in a time-dependent manner. The DNA binding activity of transcriptional factor NF-κB was quantified in myeloma cells (RPMI8226, U266, and IM-9) pretreated with 10 μmol/L ACA for the indicated times. The DNA binding activity of NF-κB in the myeloma cells was quantified by ELISA with the use of the Trans-AM NF-κB p65 Transcription Factor Assay Kit, according to the instruction of the manufacturer. Values (mean ± SD) were normalized for the cellular protein contents. *E*, ACA decreased the constitutive NF-κB activity in freshly isolated myeloma cells from two patients, but not in bone marrow mononuclear cells from a healthy donor.

mechanism of NF-κB activation, we next examined whether ACA-induced apoptosis is a result of the inhibition of NF-κB activation. ACA rapidly induced a strong decrease in the NF-κB expression in the nucleus, whereas the protein accumulated in the cytosol in RPMI8226 cells, indicating that ACA inhibited the translocation of NF-κB from the cytosol to the nucleus (Fig. 2*C*). We also confirmed the inhibitory effects of ACA on NF-κB activation by ELISA in several myeloma cell lines, as well as in primary samples from patients with multiple myeloma, but not in normal cells (Fig. 2*D* and *E*; Table 1).

1′-Acetoxychavicol acetate induced the Fas expression and down-regulation of antiapoptotic proteins in RPMI8226 cells. ACA rapidly activated caspase 8, and its specific inhibitor partially inhibited ACA-induced apoptosis in RPMI8226 cells (Fig. 2*A*). Therefore, we investigated whether or not the Fas-mediated pathway was involved in the ACA-induced apoptosis. The suppression of Fas by an antagonistic anti-Fas antibody (ZB4) dramatically inhibited ACA-induced apoptosis (Fig. 3*A*). Consistent with these results, the expression of Fas on the plasma membrane was significantly increased immediately after treatment with ACA with the induction of the Fas ligand (FasL; Fig. 3*B* and data not shown). ACA also rapidly induced the recruitment of caspase 8 to Fas-associated death domain–containing protein, suggesting that ACA induced the formation of death-inducing signaling complex (data not shown). These results indicate that the apoptotic pathway related to Fas/FasL also seems to be involved in ACA-induced apoptosis. Several studies revealed that RPMI8226 cells were resistant to Fas-mediated apoptosis because of higher levels of expression for various antiapoptotic proteins such as FLIP and XIAP. ACA down-regulated the antiapoptotic proteins FLIP and XIAP, but increased the expression of proapoptotic cytosolic AIF (Fig. 3*B*).

Effects of 1′-acetoxychavicol acetate on tumor necrosis factor α–induced sequelae in myeloma cells. TNF-α is known to activate NF-κB and have a small stimulatory effect on myeloma cell proliferation (25). However, TNF-α triggers death-receptor–mediated apoptosis in myeloma cells treated with the NF-κB inhibitor in association with the down-regulation of expression of cIAP-1. In our study, the stimulatory effect of TNF-α on the NF-κB DNA binding activity was completely inhibited by the treatment with 5 μmol/L ACA (Fig. 4*A*). TNF-α–induced apoptosis in RPMI8226 cells cotreated with a nontoxic concentration of ACA (5 μmol/L) corresponded to NF-κB inactivation (Fig. 4*B*). In addition, the treatment with TNF-α slightly up-regulated the expression of well-known NF-κB target molecules, the FLIP and XIAP proteins (Fig. 4*C*). In contrast, cotreatment with ACA and TNF-α strongly inhibited the induction of these proteins (Fig. 4*C*). In addition, ACA decreased the levels of another NF-κB target gene, the adhesion molecule ICAM, in TNF-α–treated RPMI8226 cells (Fig. 4*C*). These data further suggest that NF-κB is an important molecule for the regulation of myeloma cell adhesion and for the interaction of myeloma cells in the bone marrow microenvironment.

Activation of protein kinase C by phorbol 12-myristate 13-acetate protects cells from 1′-acetoxychavicol acetate–induced apoptosis. PMA is a tumor promoter phorbol ester recognized to be a general activator of protein kinase C (PKC; ref. 26). PMA is also known to be an NF-κB activator mediated by the induction of the nuclear translocation of NF-κB (27). A number of previous studies have reported that the activation of PKC by PMA suppresses death receptor–mediated apoptosis through the activation of NF-κB (28). In our study, pretreatment with PMA dramatically attenuated ACA-induced apoptosis by the treatment with ACA (Fig. 4*D*). In addition, pretreatment with PMA abrogated ACA-mediated caspase 8 activation and NF-κB inactivation in myeloma cells (data not shown). TLCK, a serine protease inhibitor, is known to sensitize Fas-mediated apoptosis, even in cells resistant to Fas-induced apoptosis. Several reports have also shown that TLCK can inhibit NF-κB activity by blocking PKC (29, 30). Low-dose TLCK (5 μmol/L) dramatically enhanced the apoptosis of low-dose ACA (5 μmol/L)–treated RPMI8226 cells with the activation of caspase 8 and NF-κB inactivation (Fig. 4*E*). These results also suggest that the ACA-induced apoptosis was mediated through NF-κB inactivation. In addition, low-dose MG132 (5 μmol/L), an excellent proteasome inhibitor, synergistically enhanced ACA-induced apoptosis with caspase 8 activation and NF-κB inactivation (Fig. 4*F*), strongly supporting that ACA induces the apoptosis of multiple myeloma cells through NF-κB inactivation.

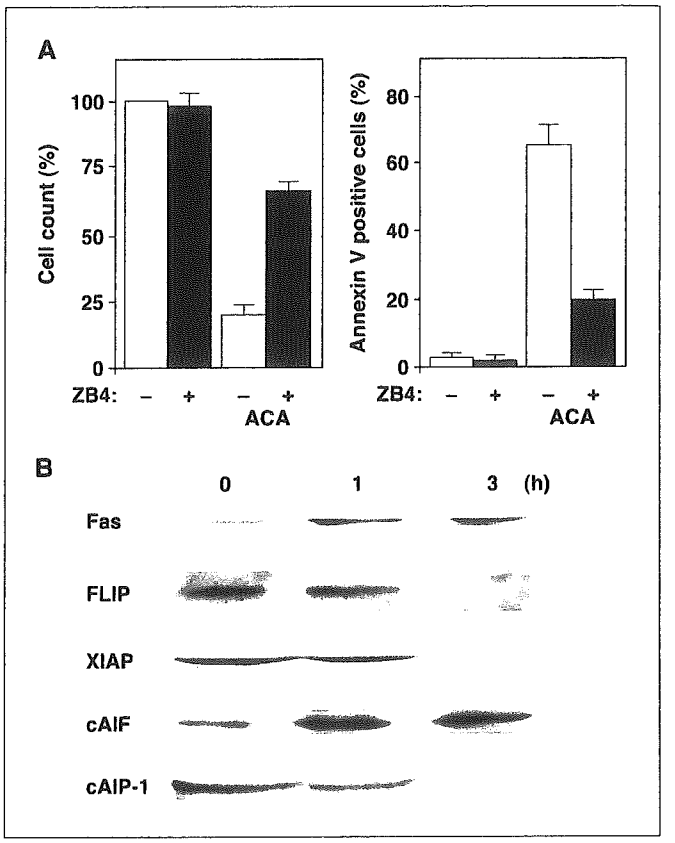

Figure 3. ACA-induced apoptosis in myeloma cells is mediated through the Fas pathway. *A*, antagonistic anti-Fas antibody (ZB4) blocks ACA-induced apoptosis in RPMI8226 cells. RPMI8226 cells were preincubated for 1 hour in the presence of 500 ng/mL of ZB4 antagonistic anti-Fas antibody, and then treated with 10 μmol/L ACA for 12 hours. Cell viability was assessed by trypan blue dye exclusion (*left*), and apoptotic cell death was analyzed by annexin V staining (*right*). *Columns*, mean of three independent experiments; *bars*, SD. *B*, expression of Fas-related proteins in ACA-treated RPMI8226 cells. The cells were treated with 10 μmol/L ACA for the indicated times. Cell lysates (15 μg of protein per lane) were fractionated on 12.5% SDS-polyacrylamide gels and analyzed by Western blotting with antibodies against Fas, FLIP, XIAP, cytosolic AIF (cAIF), and cIAP-1. Reblotting with β-actin staining showed that equal amounts of protein were presented in each lane (data not shown).

Effects of 1′-acetoxychavicol acetate *in vivo*. Our *in vitro* data prompted us to examine whether the effects of ACA are equally valid *in vivo*. Tumor weight decreased in the mice that were injected with ACA (mean weight: 0.04 ± 0.06 g in the ACA-treated group versus 0.63 ± 0.29 g in the control group; Fig. 5*A* and *B*). During treatment,

the ACA-treated mice appeared healthy. In addition, pathologic analysis at autopsy revealed no ACA-induced tissue changes in any of the organs. These results suggest that ACA had no toxic effects on the mice throughout the treatment.

Discussion

In this study, we showed for the first time that ACA, a traditional Asian condiment, induces the apoptosis of human multiple myeloma cell lines as well as of freshly obtained samples from patients with multiple myeloma through inhibition of NF-κB activity. Furthermore, ACA exhibited *in vivo* antimyeloma activity in NOD/SCID mice with no side effects. In addition, ACA did not affect the cellular growth of bone marrow cells from healthy volunteers.

Multiple myeloma is an incurable hematologic malignancy of plasma cells, despite advances in conventional chemotherapy or high-dose chemotherapy with stem cell transplantation (7–9). Therefore, novel therapeutic approaches are urgently needed in clinical settings. The recent understanding that has been gained into the biology of myeloma has led to the development of biological treatments, such as thalidomide and bortezomib, which target the myeloma cells and the bone marrow microenvironment (8, 31). In early clinical trials, these agents have shown remarkable activities against refractory multiple myeloma, but prolonged drug exposure may result in the development of *de novo* drug resistance (32, 33). Therefore, the identification and validation of additional novel targeted therapies for patients with multiple myeloma are needed. The transcription factor NF-κB has been identified as a critical component of several signal transduction pathways (34). NF-κB is an important transcription factor because of its ability to protect cells from apoptosis (35–37). Consequently, NF-κB has

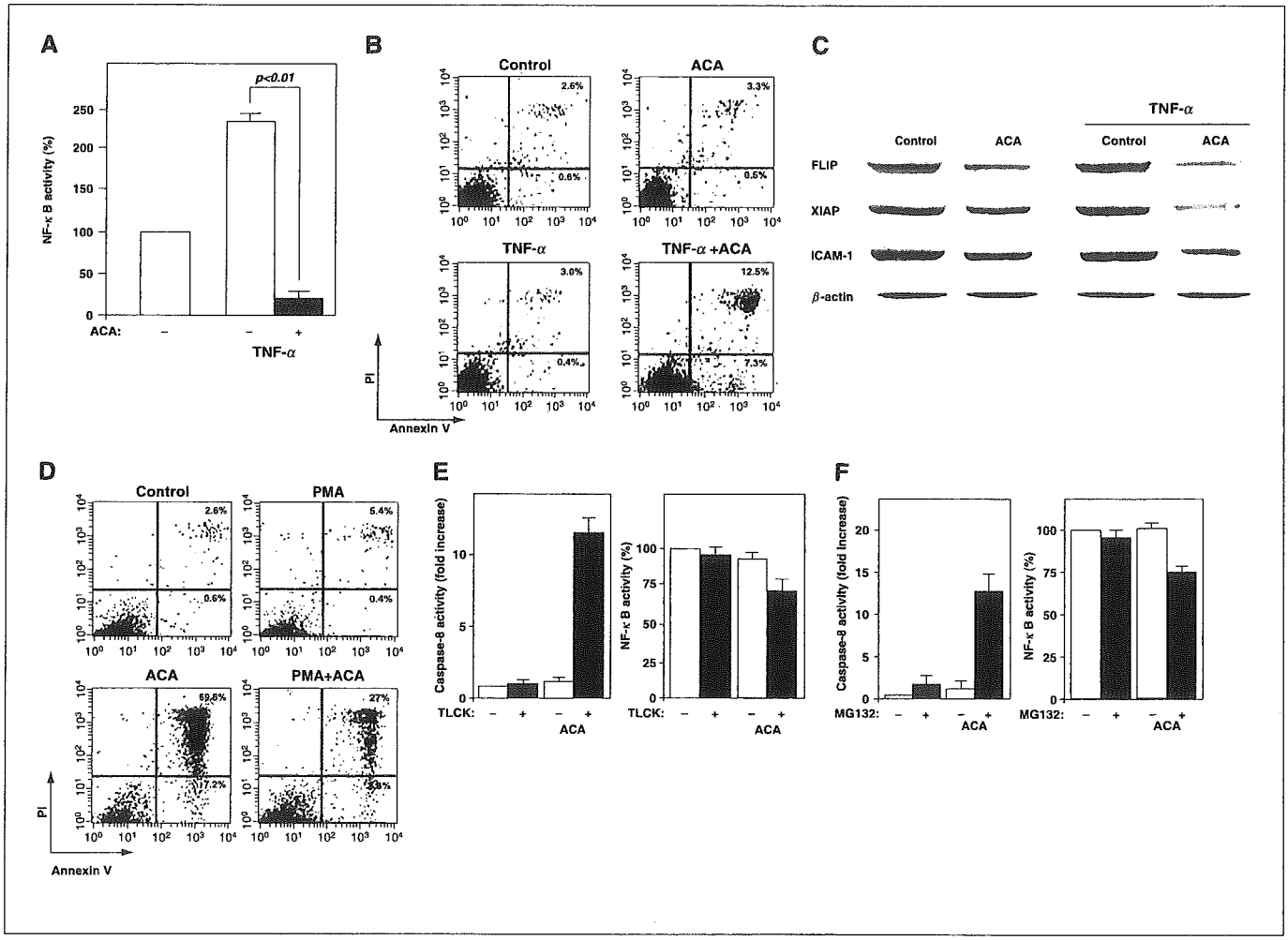

Figure 4. Effects of ACA on TNF-α–induced NF-κB activity and its sequelae in myeloma cells. RPMI8226 cells were treated with 50 ng/mL TNF-α for 12 hours, and then the cells were incubated with a nontoxic dose (5 μmol/L) of ACA for 3 hours. *A*, the DNA binding activity of NF-κB in the myeloma cells was quantified by ELISA with the use of the Trans-AM NF-κB p65 Transcription Factor Assay Kit. A nontoxic dose of ACA significantly inhibited the stimulatory effect of TNF-α on the NF-κB DNA binding activity ($P < 0.001$). *B*, the induction of apoptosis was examined by annexin V/PI double staining. Representative of three duplicate experiments. *C*, ACA inhibited the TNF-α–induced FLIP, XIAP, and ICAM-1 expressions on myeloma cells. RPMI8226 cells were incubated with 10 μmol/L ACA with or without 50 ng/mL TNF-α for 12 hours, and then cell lysates (15 μg of protein per lane) were fractionated on 12.5% SDS-polyacrylamide gels and analyzed by Western blotting. *D*, RPMI8226 cells were treated with 20 μg/mL PMA for 1 hour, and the cells were then incubated with 10 μmol/L ACA for 6 hours. Induction of apoptosis was examined by annexin V/PI double staining. *E*, RPMI8226 cells were treated with a nontoxic dose (5 μmol/L) of ACA and/or low-dose TLCL (5 μmol/L) for 24 hours. The assays for the caspase 8 activity (*left*) were analyzed by flow cytometry analysis, and the NF-κB activity (*right*) was evaluated by ELISA. *Columns*, mean of three separate experiments done in triplicate; *bars*, SD. *F*, RPMI8226 cells were treated with a nontoxic dose (5 μmol/L) of ACA with low dose (5 μmol/L) of MG132 for 24 hours. Neither agent alone in this concentration affected the cellular growth of RPMI8226 cells. The assays for the caspase 8 activity (*left*) were analyzed by flow cytometry analysis, and the NF-κB activity (*right*) was evaluated by ELISA. *Columns*, mean of three separate experiments done in triplicate; *bars*, SD.

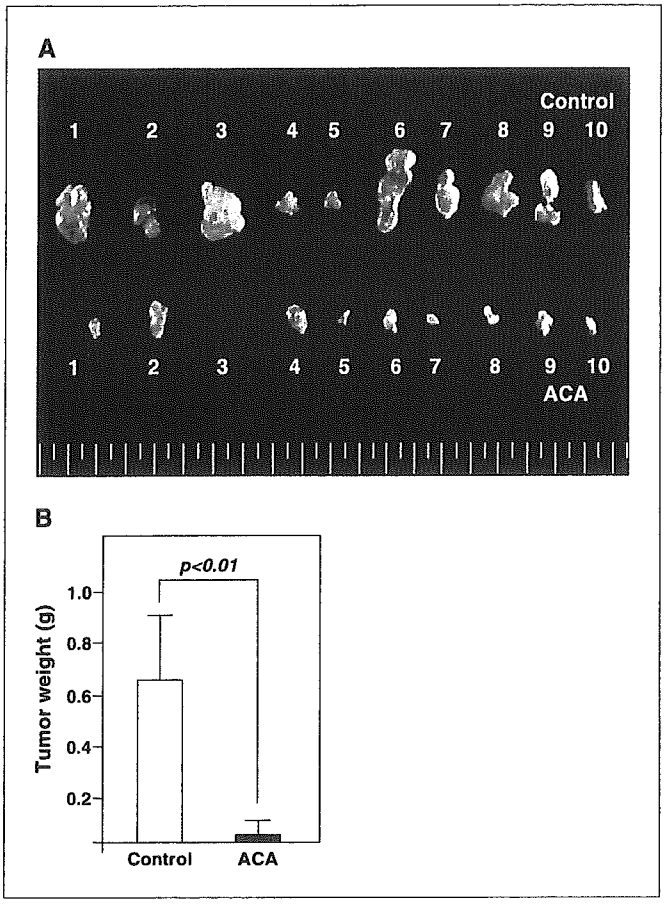

Figure 5. ACA-induced apoptosis of myeloma cells *in vivo* using NOD/SCID mice model. RPMI8226 cells (1×10^7) were inoculated s.c. into NOD/SCID mice. Seven days after transplantation, PBS (control; $n = 10$) or ACA (3 mg/kg; $n = 10$) was given i.p. once every 3 days for 2 weeks. After 2 weeks of treatment, the mice were sacrificed, and the tumor weights measured. *A*, tumors in both the control (*upper*) and ACA-treated (*lower*) mice at autopsy. *B*, ACA significantly decreased the tumor weights in the ACA-treated mice compared with the controls ($P < 0.001$).

emerged as a therapeutic target in a variety of neoplasias, and the NF-κB inhibitor induces apoptosis in myeloma cells (37). In the present study, we investigated the effects of ACA on NF-κB activity in myeloma cells *in vitro* and *in vivo*, and found for the first time that ACA inhibited NF-κB activity in multiple myeloma cell lines and patient cells, but not in normal cells. ACA also sensitized myeloma cells to TNF-α and had a synergistic proapoptotic effect with NF-κB inhibitors, MG-132 and TLCK. In contrast, an excellent NF-κB activator, PMA, dramatically abrogated ACA-induced apoptosis. These results provide the framework for targeting NF-κB inhibition by treatment with ACA in multiple myeloma therapy.

RPMI8226, U266, and IM-9 cells used in this study were relatively resistant to the NF-κB inhibitors (38) because these cells constitutively expressed higher levels of various antiapoptotic molecules including FLIP, cIAP-1, XIAP, and survivin. ACA decreased the levels of these proteins in myeloma cells. The inhibition of NF-κB stimulates caspase 9–dependent apoptosis through the reduction of XIAP and caspase 8–dependent apoptosis mediated through the decrease in FLIP. In our study, ACA activated both cascades to the caspase 8 and caspase 9 pathways in association with NF-κB inactivation, suggesting that ACA has a strong potential for inhibiting the proliferation of myeloma cells through various apoptotic signaling pathways.

The induction of NF-κB with the related up-regulation of adhesion molecules, including CD54 (ICAM-1) and CD106 (VCAM-1), has been shown in TNF-α–stimulated myeloma cell lines and bone marrow stromal cells (25, 39). In addition, myeloma cell adhesion to fibronectin mediates an antiapoptotic effect against chemotherapeutic agents (40, 41). In this study, ACA inhibited the TNF-α–induced up-regulation of the adhesion molecule ICAM-1 expression in RPMI8226 cells, suggesting that ACA may also modulate myeloma cell adhesion to stromal cells in the bone marrow. Several studies have revealed that the inhibition of NF-κB abrogates the induction of IL-6 secretion in bone marrow stromal cells and the proliferation of adherent myeloma cells (25, 39). The ACA-mediated inhibition of adhesion molecule expression, the abrogation of protection against apoptosis conferred by myeloma cells by binding to bone marrow stromal cells, and the blockade of cytokine secretion in the bone marrow milieu provide a further rationale for targeting NF-κB in novel therapies for multiple myeloma.

Finally, ACA had a synergistic proapoptotic effect with the NF-κB inhibitors MG132 and TLCK, and the NF-κB activator PMA inhibited ACA-induced apoptosis, suggesting that ACA induced apoptosis through the inhibition of NF-κB activity. The blockade of NF-κB signaling may represent a novel therapeutic strategy in multiple myeloma (7–9, 31, 32). Because NF-κB activity mediates survival and drug resistance in myeloma cells, the down-regulation of its activity by ACA, as recently observed with proteasome inhibitors (20), could also contribute to its antimyeloma activity. Our finding that ACA down-regulates the constitutive activity of NF-κB in myeloma cells further suggests that it may have combined antimyeloma activity with conventional or novel therapies that also target NF-κB.

In clinical settings, the therapeutic approach to multiple myeloma is basically chemotherapy, but severe side effects, complications, and resistance are major problems. In particular, the side effects of anticancer drugs can be fatal in elderly patients or immunocompromised patients. ACA, which is a component of a traditional Thai condiment, is a natural compound which seems to be safer than current chemotherapeutic drugs. ACA remarkably inhibited the cellular growth of myeloma cells from patients by the induction of apoptosis, whereas the same dose of ACA did not affect the cellular growth of cells from healthy volunteers, indicating that the effects of ACA are specific to malignant cells. We also showed the anticancer effects of ACA *in vivo* with no toxic effects. The Fas receptor is constitutively expressed in the liver; therefore, the liver might be very sensitive to Fas-induced apoptosis, and mice treated with an agonistic anti-CD95 antibody died from hepatic failure caused by the generalized apoptosis of hepatocytes (42). However, we could not observe any organ damage *in vivo* in our study. These results strongly indicate that it might be possible to develop ACA as a new potent anticancer agent for the management of multiple myeloma and as a novel therapeutic agent that can replace the more cytotoxic agents currently used to treat patients with multiple myeloma.

Acknowledgments

Received 1/13/2005; accepted 3/8/2005.

Grant support: Ministry of Education, Culture, Sports, Science and Technology of Japan (M. Kizaki), and a grant from the Mitsubishi Pharma Research Foundation (M. Kizaki).

The costs of publication of this article were defrayed in part by the payment of page charges. This article must therefore be hereby marked *advertisement* in accordance with 18 U.S.C. Section 1734 solely to indicate this fact.

We thank Kaori Saito for her excellent technical assistance.

References

1. Kondo A, Ohigashi H, Murakami A, Jiwajinda S, Koshimizu K. A potent inhibitor of tumor promoter-induced Epstein-Barr virus activation, 1′-acetoxychavicol acetate from Languas galanga, a traditional Thai condiment. Biosci Biotechnol Biochem 1993;57: 1344–5.
2. Ohnishi M, Tanaka T, Makita H, et al. Chemopreventive effect of a xanthine oxidase inhibitor, 1′-acetoxychavicol acetate, on rat oral carcinogenesis. Jpn J Cancer Res 1996;87:349–56.
3. Moffatt J, Hashimoto M, Kojima A, et al. Apoptosis induced by 1′-acetoxychavicol acetate in Ehrlich ascites tumor cells is associated with modulation of polyamine metabolism and caspase-3 activation. Carcinogenesis 2000;21:2151–7.
4. Nakamura Y, Murakami A, Ohto Y, Torikai K, Tanaka T, Ohigashi H. Suppression of tumor promoter-induced oxidative stress and inflammatory responses in mouse skin by a superoxide generation inhibitor 1′-acetoxychavicol acetate. Cancer Res 1998;58:4832–9.
5. Tanaka T, Makita H, Kawamori T, et al. A xanthine oxidase inhibitor 1′-acetoxychavicol acetate inhibits azoxymethane-induced colonic aberrant crypt foci in rats. Carcinogenesis 1997;18:1113–8.
6. Ito K, Nakazato T, Murakami A, et al. Induction of apoptosis in human myeloid leukemic cells by 1′-acetoxychavicol acetate through a mitochondrial- and Fas-mediated dual mechanism. Clin Cancer Res 2004; 10:2120–30.
7. Hideshima T, Anderson KC. Molecular mechanisms of novel therapeutic approaches for multiple myeloma. Nat Rev Cancer 2002;2:927–37.
8. Sirohi B, Powles R. Multiple myeloma. Lancet 2004;363:875–87.
9. Hideshima T, Bergsagel PL, Kuehl WM, Anderson KC. Advances in biology of multiple myeloma: clinical applications. Blood 2004;104:607–18.
10. Bendall HH, Sikes ML, Ballard DW, Oltz EM. An intact NF-κB signaling pathway is required for maintenance of mature B cell subsets. Mol Immunol 1999; 36:187–95.
11. Doerre S, Corley RB. Constitutive nuclear transcription of NF-κB in B cells in the absence of IκB degradation. J Immunol 1999;169:269–77.
12. Baldwin AS Jr. The NF-κB and IκB proteins: new discoveries and insights. Annu Rev Immunol 1996;14: 649–81.
13. Ghosh S, May MJ, Kopp EB. NF-κB and Rel proteins: evolutionarily conserved mediators of immune responses. Annu Rev Immunol 1998;16:225–60.
14. DiDonato JA, Mercurio F, Karin M. Phosphorylation of IκBα precedes but is not sufficient for its dissociation from NF-κB. Mol Cell Biol 1995;15:1302–11.
15. Feinman R, Koury J, Thames M, Barlogie B, Epstein J, Siegel DS. Role of NF-κB in the rescue of multiple myeloma cells from glucocorticoid-induced apoptosis by bcl-2. Blood 1999;93:3044–52.
16. Ni H, Ergin M, Huang Q, et al. Analysis of expression of nuclear factor κB (NF-κB) in multiple myelom: down-regulation of NF-κB induces apoptosis. Br J Haematol 2001;115:279–86.
17. Chauhan D, Uchiyama H, Akbarali Y, et al. Multiple myeloma cell adhesion-induced interleukin-6 expression in bone marrow stromal cells involves activation of NF-κB. Blood 1996;87:1104–12.
18. Keifer JA, Guttridge DC, Ashburner BP, Baldwin AS Jr. Inhinbition of NF-κB activity by thalidomide through suppression of IκB kinase activity. J Biol Chem 2001;276: 22382–7.
19. Palombella VJ, Conner EM, Fuseler JW, et al. Role of the proteasome and NF-κB in streptococcal cell wall-induced polyarthritis. Proc Natl Acad Sci U S A 1998;95: 15671–6.
20. Hideshima T, Richardson P, Chauhan D, et al. The proteasome inhibitor PS-341 inhibits growth, induces apoptosis, and overcomes drug resistance in human multiple myeloma. Cancer Res 2001;61:3071–6.
21. Hideshima T, Chauhan D, Richardson P, et al. NF-κB as a therapeutic target in multiple myeloma. J Biol Chem 2002;277:16639–47.
22. Murakami A, Toyota K, Okura S, Koshimizu K, Ohigasgi H. Structure-activity relationships of (1′*S*)-1′-acetoxychavichol acetate, a major constituent of a Southeast Asia condiment plant Langus galangal, on the inhibition of tumor-promoter-induced Epstein-Barr virus activation. J Agric Food Chem 2000;48: 1518–23.
23. Ito K, Nakazato T, Yamato K, et al. Induction of apoptosis in leukemic cells by homovanillic acid derivative, capsaicin, through oxidative stress: implication of phosphorylation of p53 at Ser-15 residue by reactive oxygen species. Cancer Res 2004;64:1071–8.
24. Workman P, Balman A, Hickman JA, et al. UKCCCR guidelines for the welfare of animals in experimental neoplasia. Br J Cancer 1998;58:109–13.
25. Hideshima T, Chauhan D, Schlossman R, Richardson P, Anderson KC. The role of tumor necrosis factor α in the pathophysiology of human multiple myeloma: therapeutic applications. Oncogene 2001;20:4519–27.
26. Kvanta A, Jondal M, Fredholm BB. Translocation of the α- and β-isoforms of protein kinase C following activation of human T-lymphocytes. FEBS Lett 1991;283: 321–4.
27. Epinat JC, Gilmore TD. Diverse agents act at multiple levels to inhibit the Rel/NF-κB signal transduction pathway. Oncogene 1999;18:6896–909.
28. Meng XW, Heldebrant MP, Kaufman SH. Phorbol 12-myristate 13-acetate inhibits death receptor-mediated apoptosis in Jurkat cells by disrupting recruitment of Fas-associated polypeptide with death domain. J Biol Chem 2002;277:3776–83.
29. Lee Y, Shacter E. Fas aggregation does not correlate with Fas-mediated apoptosis. J Immunol 2001;167:82–9.
30. Solomon DH, O'Brian CA, Weinstein IB. *N*-α-Tosyl-L-lysine chloromethyl ketone and *N*-α-tosyl-L-phenylalanine chloromethyl ketone inhibit protein kinase C. FEBS Lett 1985;190:342–4.
31. Bruno B, Rotta M, Giaccone L, et al. New drugs for treatment of multiple myeloma. Lancet Oncol 2004;5: 430–42.
32. Hideshima T, Richardson P, Anderson KC. Novel therapeutic approaches for multiple myeloma. Immunol Rev 2003;194:164–76.
33. Bartlett JB, Dredge K, Dalgleish AG. The evolution of thalidomide and its IMiD derivatives as anticancer agents. Nat Rev 2004;4:314–22.
34. Barnes PJ, Karin M. Nuclear factor-κB: a pivotal transcription factor in chronic inflammatory diseases. N Engl J Med 1997;336:1066–71.
35. Wang CY, Mayo MW, Baldwin AS Jr. TNF- and cancer therapy-induced apoptosis: potentiation by inhibition of NF-κB. Science 1996;274:784–7.
36. Van Antwerp DJ, Martin SJ, Kafri T, Green DR, Verma IM. Suppression of TNF-α-induced apoptosis by NF-κB. Science 1996;274:787–9.
37. Beg AA, Ruben SM, Scheinman RI, Haskill S, Rosen CA, Baldwin AS Jr. IκB interacts with the nuclear localization sequences of the subunits of NF-κB: a mechanism for cytoplasmic retention. Genes Dev 1992; 6:1899–913.
38. Bharti A, Donato N, Singh S, Aggarwal BB. Curcumin (diferuloylmethane) down-regulates the constitutive activation of nuclear factor-κB and IκBα kinase in human multiple myeloma cells, leading to suppression of proliferation and induction of apoptosis. Blood 2003; 101:1053–62.
39. Hideshima T, Chauhan D, Podar K, Schlossman R, Richardson P, Anderson KC. Novel therapies targeting the myeloma cell and its bone marrow microenvironment. Semin Oncol 2001;28:607–12.
40. Nov H, Holt RU, Rø TB, et al. A selective c-Met inhibitor blocks an autocrine Hepatocyte Growth Factor loop in ANBL-6 cells and prevents migration and adhesion of myeloma cells. Clin Cancer Res 2004;10: 6686–94.
41. Dai Y, Pei X-Y, Rahmani M, Conrad DH, Dent P, Grant S. Interuption of the NF-κB pathway by Bay 11-7082 promotes UCN-01-mediated mitochondrial dysfunction and apoptosis in human multiple myeloma cells. Blood 2004;103:2761–70.
42. Kondo T, Suda T, Fukuyama H, Adachi M, Nagata S. Essential role of the Fas ligand in the development of hepatitis. Nat Med 1997;3:409–13.

J Bone Miner Metab (2005) 23:270–273
DOI 10.1007/s00774-004-0595-y

SHORT COMMUNICAITON

Ryoji Fujimaki · Katsuhiko Hayashi · Naoko Watanabe
Taketo Yamada · Yoshiaki Toyama · Ken-ichi Tezuka
Nobumichi Hozumi

Expression of Cre recombinase in the mouse developing chondrocytes driven by the mouse α2(XI) collagen promoter

Received: June 14, 2004 / Accepted: October 26, 2004

Key words Cre-LoxP · Chondrocyte · α2(XI) collagen gene

Introduction

Endochondral bone formation is a highly coordinated process of skeletal development, through which all the longitudinal bones are created. Endochondral bone formation is initiated with the condensation of mesenchymal cells. Then, aggregated mesenchymal cells subsequently differentiate into cartilage, and later primordial cartilages are replaced by bone. Thus, considering the fact that chondrogenesis precedes bone formation in endochondral bone formation, investigation of chondrogenesis provides the key to understanding the molecular mechanisms involved in skeletogenesis.

Targeted gene deletion (gene knockout) technology is versatile in the fields of skeletal biology. However, the conventional gene knockout approach sometimes leads to embryonic lethality before bone formation, and the problem makes it difficult to elucidate the function of genes. The Cre-loxP system was established to overcome this limitation. The Cre-loxP system enables us to design experiments to disrupt genes in a time- and site-specific manner, and it is becoming a powerful tool for analyzing gene function in vivo. This system is based on the principle that the bacteriophage P1 Cre recombinase recognizes the specific sequences, called loxP sites, and excises the DNA floxed by the two loxP sites. Two mouse lines are required for the conditional gene deletion experiment: a mouse strain carrying a target gene flanked by two loxP sites, and a conventional transgenic mouse strain expressing Cre recombinase under the control of a transgenic promoter. Mating of these two mouse lines results in Cre-mediated gene disruption only within the cells in which the promoter is activated, and Cre recombinase is expressed.

Type XI collagen, which is one of the structural components of the cartilage matrix, is constituted by three distinct subunits: α1(XI), α2(XI), and α3(XI). Type XI collagen plays a critical role in regulating the formation of the collagen fibrils. Chondrodysplasia in *cho/cho* mice is caused by a mutation in the α1(XI) gene [1]. It has been also reported that mutations in the α2(XI) gene cause chondrodysplasias in humans, such as Stickler syndrome [2]. Although the α1(XI) and α3(XI) genes are expressed in many tissues other than cartilage, expression of the mouse α2(XI) gene is more restricted to cartilage [3–5], and the 5′-flanking region of the α2(XI) collagen gene has been documented by Tsumaki et al. [6]. They demonstrated that the upstream 742-bp sequence of the transcriptional start site of the α2(XI) collagen gene contained genetic elements required for specific expression in cartilage.

We generated Cre-expressing transgenic mice under the control of the −742-bp promoter sequence of the mouse α2(XI) collagen gene. In this article, we report the establishment of a mouse line that expresses Cre recombinase driven by the α2(XI) collagen promoter and show this mouse line will be a useful tool for analyzing the role of various genes involved in the complicated process of chondrogenesis.

R. Fujimaki · N. Watanabe · N. Hozumi (✉)
Research Institute for Biological Sciences, Tokyo University of Science (RIKADAI), 2669 Yamazaki, Noda 278-0022, Japan
Tel. +81-4-7121-4091; Fax +81-4-7121-4099
e-mail: nobhozmi@rs.noda.tus.ac.jp

K. Hayashi
Department of Molecular Embryology Research Institute, Osaka Medical Center for Maternal and Child Health, Osaka, Japan

T. Yamada
Department of Pathology, Keio University School of Medicine, Tokyo, Japan

R. Fujimaki · Y. Toyama
Department of Orthopaedic Surgery, Keio University School of Medicine, Tokyo, Japan

K. Tezuka
Department of Tissue and Organ Development, Gifu University Graduate School of Medicine, Gifu, Japan

Materials and methods

DNA construction and production of transgenic mice

The transgenic construct was generated from Pnass-lacZ–Int (gift from Dr. N. Tsumaki) [6], which carries the −742-bp promoter sequence of the mouse α2(XI) collagen gene, SV40 RNA splice site, β-galactosidase gene, SV40 polyadenylation signal, and the first intron of the mouse α2(XI) collagen gene. The β-galactosidase gene was replaced with the Cre gene. The 4.1-kb construct was linearized and microinjected into pronuclei of fertilized BDF1(C57BL/6xDBA2) zygotes according to standard procedures [7].

Polymerase chain reaction analysis and Southern blots

The transgenes were identified by polymerase chain reaction (PCR) and Southern blots on tail and placenta genomic DNA. For PCR analysis, the primers used for Cre gene were Cre-5′, 5′-CCTGGAAAATGCTTCTGTCCGTTT GCC-3′; Cre-3′, 5′-GAGTTGATAGCTGGCTGGTGG CAGATG-3′, as described [8]. For Southern blot analysis, tail DNA were digested with *Xho*I, fractionated on 0.8% agarose gel, transferred to a nylon membrane (Hybond-N; Amersham-Pharmacia Biotech, Tokyo, Japan) and probed with an 0.6-kb, digoxigenin (DIG)-labeled PCR fragment of Cre gene.

X-gal staining and histology

Embyos and neonates were fixed with 2% paraformaldehyde and 0.2% glutaraldehyde for 1 h at 4°C, washed three times with phosphate-buffered saline (PBS), and incubated in staining solutions [1 mg/ml 5-bromo-4-chloro-3-indolyl β-D-galactopyranoside (X-gal), 4 mM $K_4Fe(CN)_6$, 4 mM $K_3Fe(CN)_6$, 2 mM $MgCl_2$ in PBS] at 37°C overnight. Specimens were embedded in wax, sectioned, and counterstained with eosin or kernechtrot.

Results and discussion

The Cre recombinase gene was placed downstream of the −742-bp promoter sequence of the mouse α2(XI) collagen gene. The first intron of the α2(XI) collagen gene was placed at the 3′-end of the Cre gene, which is also responsible for cartilage-specific expression (Fig. 1A). Transgene integration in the mouse genome was assessed by genomic PCR and Southern blot using tail DNA extracts (Fig. 1B,C). Five different founder lines were obtained.

These five transgenic mouse lines were crossed with another transgenic mouse line, CAG-CAT-Z, carrying a reporter gene constructed to examine whether the founder lines express sufficiently high Cre recombinase to mediate recombination at loxP sites and reveal the spatiotemporal expression patterns of the gene. The CAG-CAT-Z mouse

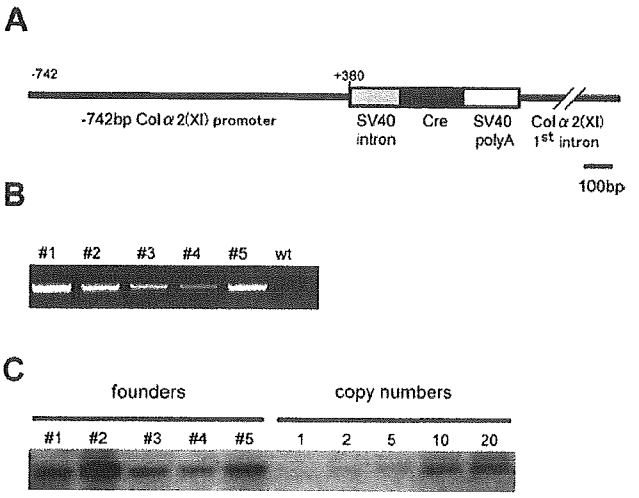

Fig. 1. A Schematic diagram of the DNA construct. The Cre recombinase gene was placed under the control of the −742 bp promoter sequence and the first intron of the mouse α2(XI) collagen gene. **B** Founder lines are genotyped by polymerase chain reaction (PCR) using Cre-specific primers. **C** Determination of the copy numbers of founders by quantitative Southern blot

directs expression of the LacZ gene upon Cre-mediated recombination of the loxP-flanked chloramphenicol acetyltransferase (CAT) gene located between the CAG promoter and the lacZ gene [9]. Embryos were stained with X-gal to detect β-gal activity.

Founder line #2 showed Cre activity in chondrocytes, parts of the brain, and neural tubes (data not shown). The −518-bp and −530-bp promoter sequences of the α2(XI) collagen gene direct artificial expression in neural tissues [10]. We speculated that the promoter region of the transgene in founder line #2 was partially shortened physically or functionally during transgene integration and directed expression of Cre in neural tissues. Founder line #3 showed Cre activity in the whole body. This expression pattern, which cannot be explained by the previous studies [6,10], might be due to position effects at the site of transgene integration in the genome. Founder lines #1 and #5 failed to demonstrate Cre recombinase activity.

Founder line #4 revealed a desirable result for our purpose, although copy numbers of the transgene were the smallest among the five founder lines (Fig. 1C). Embryos (founder line #4 × CAG-CAT-Z F1) showed weak β-gal activity in the notochord at 11.0 days postcoitum (dpc) (Fig. 2A). By 12.5 dpc, lacZ expression was evident in primordial cartilages of forelimb and notochord remnant (Fig. 2B). Histological sections of the radius and ulna revealed that LacZ was uniformly expressed in every chondrocyte of primordial cartilages (Fig. 2C). Cre has not yet been expressed in mesenchymal condensation areas of the forefoot plate, which are supposed to become chondrocytes in later stages (Fig. 2D). By 14.5 dpc, β-gal activity was observed in the endochondral bone formation areas such as forelimbs and hindlimbs, ribs, scapula, and vertebrae (Fig. 2E). No lacZ staining was visible in any tissues other than cartilages. In the 2-day-old neonate, lacZ staining was also visible in other

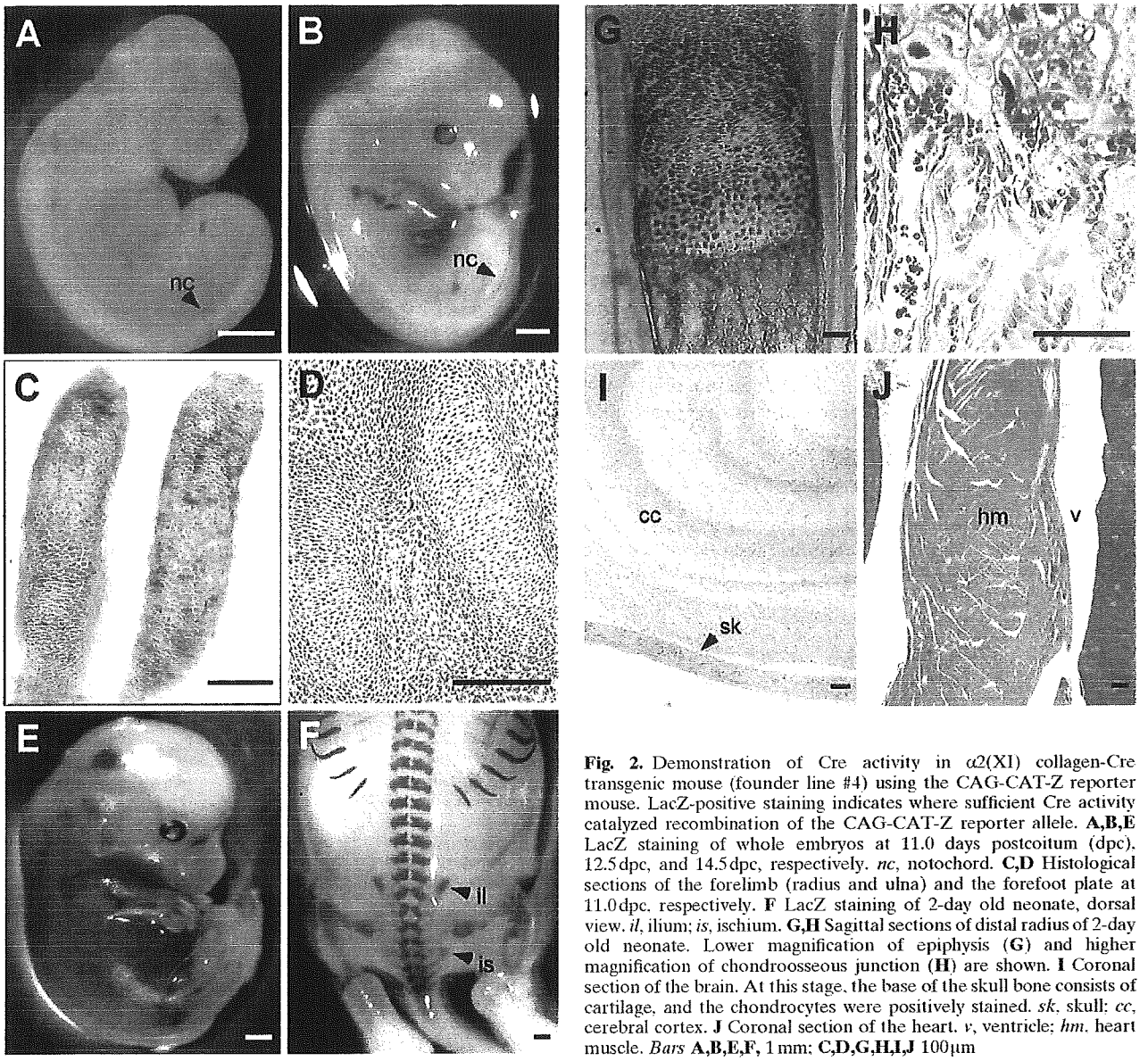

Fig. 2. Demonstration of Cre activity in α2(XI) collagen-Cre transgenic mouse (founder line #4) using the CAG-CAT-Z reporter mouse. LacZ-positive staining indicates where sufficient Cre activity catalyzed recombination of the CAG-CAT-Z reporter allele. **A,B,E** LacZ staining of whole embryos at 11.0 days postcoitum (dpc), 12.5 dpc, and 14.5 dpc, respectively. *nc*, notochord. **C,D** Histological sections of the forelimb (radius and ulna) and the forefoot plate at 11.0 dpc, respectively. **F** LacZ staining of 2-day old neonate, dorsal view. *il*, ilium; *is*, ischium. **G,H** Sagittal sections of distal radius of 2-day old neonate. Lower magnification of epiphysis (**G**) and higher magnification of chondroosseous junction (**H**) are shown. **I** Coronal section of the brain. At this stage, the base of the skull bone consists of cartilage, and the chondrocytes were positively stained. *sk*, skull; *cc*, cerebral cortex. **J** Coronal section of the heart. *v*, ventricle; *hm*, heart muscle. *Bars* **A,B,E,F,** 1 mm; **C,D,G,H,I,J** 100 μm

endochondral formation areas, such as the ilium, ischium (Fig. 2F) and base of the skull (Fig. 2I). Histological sections of the distal radius of the neonate demonstrated that β-gal activity was observed in all epiphyseal chondrocytes throughout their differentiation stages, from resting to hypertrophic chondrocytes (Fig. 2G). No lacZ staining was detected in the cuboidal osteoblastic cells lining on the cancellous bone (Fig. 1H). We also noted that the #4 transgenic mouse is fertile and viable, implying that the transgene does not disrupt a vital endogenous gene. The activity of the Cre transgene did not change in the offspring mice of founder line #4. This expression pattern of the #4 mouse line was almost identical to that of the previously reported transgenic mouse that directed lacZ expression under the control of the −742-bp promoter [6].

As a chondrocyte-specific Cre-expressing transgenic mouse, the α2(II) collagen promoter directed Cre-expressing mice were previously reported [11,12]. Cre activity was noted in tissues other than cartilage such as heart and osteoblasts, and a small amount of mosaicism in Cre activity was observed in the cartilage. In contrast, we did not detect Cre expression in noncartilage tissues, including heart, brain, and osteoblasts (Fig. 2H–J), except for the notochord, and Cre was uniformly expressed in all chondrocytes we examined. Generally, the expression level of α2(II) collagen is higher than that of α2(XI) collagen, and this may cause more specific Cre recombinase expression in the cartilage of α2(XI)-Cre mice. Therefore, this transgenic mouse line would become an appropriate alternative for the analysis of gene function in chondrogenesis.

Summary

Spatial and temporal gene inactivation by the cre-loxP system is a powerful tool for analyzing genes of interests. We generated a transgenic mouse line that expresses Cre recombinase under the control of the −742-bp promoter sequence of the mouse α2(XI) collagen gene. Crossing this mouse line with a reporter mouse revealed that Cre recombinase activity is observed specifically in developing chondrocytes. This chondrocyte-specific Cre expression was observed from the early stage of chondrocyte differentiation in forelimb at 12.5 dpc, but not expressed in mesenchymal condensations. This transgenic mouse line will be a suitable resource for the analysis of gene function in differentiating chondrocytes and the mechanism of endochondral ossification.

Acknowledgments We thank Dr. Noriyuki Tsumaki for his generous gift for the α2(XI) collagen gene promoter/enhancer construct, Dr. Jun-ichi Miyazaki for providing us with the CAG-CAT-Z, mouse and Dr. Takeshi Miyamoto for technical help. This work was supported in part by grants from the Ministry of Education, Culture, Sports, Science and Technology of Japan.

References

1. Li Y, Lacerda DA, Warman ML, Beir DR, Yoshioka H, Ninomiya Y, Oxford JT, Morris NP, Andrikopoulos K, Ramirez F, Wardell BB, Lifferth GD, Teusher C, Woodward SR, Taylor BA, Seegmiller RE, Olsen BR (1995) A fibrillar collagen gene, Col11a1, is essential for skeletal morphogenesis. Cell 80:423–430
2. Vikkula M, Mariman EC, Lui VC, Zhidkova NI, Tiller GE, Goldring MB, Van Beersum SE, de Waal Malefijt MC, van den Hoogen FH, Ropers HH, Mayne R, Cheah KS, Olsen BR, Warman ML, Brunner HG (1995) Autosomal dominant and recessive osteochondrodysplasias associated with the COL11A2 locus. Cell 80:431–437
3. Yoshioka H, Iyama K, Khaleduzzaman M, Ninomiya Y, Ramirez F (1995) Developmental pattern of expression of the mouse alpha 1 (XI) collagen gene (Col11a1). Dev Dyn 204:41–47
4. Tsumaki N, Kimura T (1995) Differential expression of an acidic domain in the amino-terminal propeptide of mouse pro-alpha 2(XI) collagen by complex alternative splicing. J Biol Chem 270: 2372–2378
5. Sugimoto M, Kimura T, Tsumaki N, Matsui Y, Nakata K, Kawahata H, Yasui N, Kitamura Y, Nomura S, Ochi T (1998) Differential in situ expression of alpha2(XI) collagen mRNA isoforms in the developing mouse. Cell Tissue Res 292:325–332
6. Tsumaki N, Kimura T, Matsui Y, Nakata K, Ochi T (1996) Separable cis-regulatory elements that contribute to tissue- and site-specific α2(XI) collagen gene expression in the embryonic mouse cartilage. J Cell Biol 134:1573–1582
7. Hogan B, Beddington R, Constantini F, Lacy E (1994) Manipulating the Mouse Embryo: A Laboratory Manual, 2nd edn. Cold Spring Harbor Laboratory Press, Cold Spring Harbor, NY
8. Dacquin R, Starbuck M, Schinke T, Karsenty G (2002) Mouse alpha1(I)-collagen promoter is the best known promoter to drive efficient Cre recombinase expression in osteoblast. Dev Dyn 224:245–251
9. Sakai K, Miyazaki J (1997) A transgenic mouse line that retains Cre recombinase activity in mature oocytes irrespective of the cre transgene transmission. Biochem Biophys Res Commun 237:318–324
10. Tsumaki N, Kimura T, Tanaka K, Kimura JH, Ochi T, Yamada Y (1998) Modular arrangement of cartilage- and neural tissue-specific cis-elements in the mouse α2(XI) collagen promoter. J Biol Chem 273:22861–22864
11. Ovchinnikov DA, Deng JM, Ogunrinu G, Behringer RR (2000) Col2a1-directed expression of Cre recombinase in transgenic mice. Genesis 26:145–146
12. Sakai K, Hiripi L, Glumoff V, Brandau O, Eerola R, Vuorio E, Bosze Z, Fassler R, Aszodi A (2001) Stage- and tissue-specific expression of a Col2a1-Cre fusion gene in transgenic mice. Matrix Biol 19:761–767

Catechin, a green tea component, rapidly induces apoptosis of myeloid leukemic cells via modulation of reactive oxygen species production *in vitro* and inhibits tumor growth *in vivo*

Tomonori Nakazato
Keisuke Ito
Yoshitaka Miyakawa
Kentaro Kinjo
Taketo Yamada
Nobumichi Hozumi
Yasuo Ikeda
Masahiro Kizaki

Background and Objectives. The aim of this study was to investigate the possibility of green tea polyphenol, (-)-epigallocatechin-3-gallate (EGCG) as a novel therapeutic agent for patients with myeloid leukemia.

Design and Methods. We investigated the effects of EGCG on the induction of apoptosis in leukemic cells *in vitro* and *in vivo*. We further examined the molecular mechanisms of EGCG-induced apoptosis in myeloid leukemic cells.

Results. EGCG rapidly induced apoptotic cell death in retinoic acid (RA)-resistant acute promyelocytic leukemia (APL), UF-1 cells within 3 h. EGCG-induced apoptosis in UF-1 cells was associated with the loss of mitochondrial transmembrane potentials ($\Delta\Psi_m$) and activation of caspase-3 and -9. Elevation of intracellular reactive oxygen species (ROS) production was also demonstrated during EGCG-induced apoptosis of UF-1 as well as fresh myeloid leukemic cells. In NOD/SCID mice transplanted with UF-1 cells, EGCG effectively inhibited tumor growth *in vivo*, and the number of mitoses among the cells significantly decreased in comparison to the number in control mouse cells.

Interpretation and Conclusions. In summary, EGCG has potential as a novel therapeutic agent for myeloid leukemia via induction of apoptosis mediated by modification of the redox system.

Key words: green tea, catechin, apoptosis, leukemic cells, reactive oxygen species.

Haematologica 2005; 90:317-325

From the Division of Hematology, Department of Internal Medicine (TN, KI, YM, KK, YI, MK) and Pathology, Keio University School of Medicine, Tokyo, Japan (TY); Institute of Biological Science, Science University of Tokyo, Chiba, Japan (NH).

Correspondence:
Masahiro Kizaki, M.D., Division of Hematology, Department of Internal Medicine, Keio University School of Medicine, 35 Shinanomachi, Shinjuku-ku, Tokyo 160-8582, Japan.
E-mail: makizaki@sc.itc.keio.ac.jp

Recently, green tea has attracted much attention because of its beneficial health effects; the polyphenolic compounds present in green tea include (-)-epigallocatechin-3-gallate (EGCG), (-)-epicatechin-3-gallate (ECG), (-)-epigallocatechin (EGC), and epicatechin (EC), which have been shown to have cancer preventive effects in many animal tumor models.[1] In fact, epidemiologic studies have shown that green tea consumption can reduce the incidence of cancer and metastases.[2-6] Green tea has unique characteristics as an agent and has few adverse effects. In addition, it is inexpensive, can be consumed orally, and has a long history as a generally tolerated beverage among all races. Therefore, green tea appears to have the potential of becoming an ideal agent for chemoprevention.[7] Moreover, EGCG has been shown to induce G_0/G_1 phase cell cycle arrest in human epidermoid carcinoma cells, thereby inhibiting proliferation and inducing apoptosis in many cancer cells *in vitro*.[7-9] The therapeutic approach to acute leukemia is basically chemotherapy to achieve complete remission, based on the concept of *total cell killing*.[10] However, severe side effects and complications such as serious infections and bleeding due to anti-cancer drugs are major problems in the clinical setting. In addition, repeated episodes of relapse of the disease may lead to refractory or chemotherapy-resistant leukemia. The clinical evidence thus suggests the limitations of leukemia chemotherapy; novel effective therapeutic approaches with less toxicity are therefore actively being sought. Differentiation-inducing therapy employing a physiologically active derivative of vitamin A, all-*trans* retinoic acid (ATRA), brought remarkable advances in the therapeutic outcomes of acute promyelocytic leukemia (APL) at the end of the last century.[11] However, the clinical remission due to ATRA is of short duration, and most patients who receive continuous treatment with ATRA develop RA-resistant diseases.[12] Therefore, investigators have actively sought out new agents with the ability to stimulate cellular differentiation and induce apoptosis in the types of cells associated with acute leukemia.

Design and Methods

Cells and cell culture

The RA-resistant APL cell line UF-1 was established in our laboratory from a patient with relapsed APL who had received ATRA,[13] and the RA-sensitive NB4 promyelocytic leukemia cell line was a gift from Dr. M. Lanotte (Hôpital St Louis, Paris, France).[14] The human myeloid leukemic cell lines HL-60, U937, K562, and KU812 were obtained from the Japan Cancer Research Resources Bank (Tokyo, Japan). Bone marrow or peripheral blood samples from 6 newly diagnosed patients with acute myelogenous leukemia (AML) were obtained according to appropriate Human Protection Committee validation and with informed consent. Mononuclear cells were separated by Lymphoprep (Nycomed Pharma As, Oslo, Norway). The percentage of leukemic blast cells was more than 80% of the mononuclear cells. Cells were maintained in RPMI 1640 medium (GIBCO-BRL, Gaitherburg, MD, USA) with 15% fetal calf serum (Hyclone Laboratories, Logan, MT, USA), 100 U/mL penicillin, and 100 mg/mL streptomycin in a humidified atmosphere with 5% CO_2.

Reagents

Various catechin derivatives, including EC, ECG, EGC, and EGCG, were purchased from WAKO Chemical Co. (Tokyo, Japan). Catechin derivatives were dissolved in DMSO and none of the cultures contained more than 0.1% DMSO. Controls were run using 0.1% DMSO and this concentration of diluent had no effect. N-acetyl-L-cysteine (NAC), rotenone, and myxothiazol were obtained from Sigma Chemical Co. (St. Louis, MO, USA).

Assays for apoptosis

Apoptotic cells were quantified by annexin V-FITC and propidium iodide (PI) double staining using a staining kit purchased from PharMingen (San Diego, CA, USA). In addition, induction of apoptosis was detected by a DNA fragmentation assay. The mitochondrial transmembrane potential ($\Delta\psi_m$) was determined by flow cytometry (FACS Calibur; Becton Dickinson, San Jose, CA, USA). Briefly, cells were washed twice with PBS and incubated with 1 μg/mL rhodamine 123 (Sigma) at 37° for 30 min. Rhodamine 123 intensity was determined by flow cytometry.

Cell cycle analysis

Cells (1×10^6) were suspended in hypotonic solution (0.1% Triton X-100, 1 mM Tris-HCl (pH 8.0), 3.4 mM sodium citrate, 0.1 mM EDTA) and stained with 50 μg/mL of PI. The DNA content was analyzed by flow cytometry. The population of cells in each cell cycle phase was determined using ModiFIT software (Becton Dickinson).

Caspase assays

In the caspase inhibitor assay, cells were pretreated with a synthetic pan-caspase inhibitor (20 μM, Z-VAD-FMK) or caspase-3 inhibitor (50 μM, DEVD-CHO), and caspase-8 and -9 inhibitors (50 μM, Z-IETD-FMK and LEHD-CHO, respectively) for 2 h prior to addition of EGCG (100 μM). All inhibitors were purchased from Calbiochem (La Jolla, CA, USA).

Measurement of intracellular generation of ROS

To assess the generation of reactive oxygen species (ROS), control and EGCG-treated cells were incubated with 5 μM DHE (Molecular Probes, Eugene, OR, USA), which is oxidized to the fluorescent intercalator, ethidium, by cellular oxidants, particularly superoxide radicals. Cells (5×10^5) were stained with 5 μM DHE for 30 min at 37°C, and were then washed and resuspended in PBS. The oxidative conversion of DHE to ethidium was measured by flow cytometry (Becton Dickinson).

Cell lysate preparation and Western blotting

Cells were collected by centrifugation at 700 g for 10 min and then the pellets were resuspended in lysis buffer (1% NP-40, 1 mM phenylmethylsulfonyl fluoride (PMSF), 40 mM Tris-HCl (pH8.0), 150 mM NaCl) at 4°C for 15 min. For the detection of PML/RARα, cells were extracted by the method of Yoshida *et al.*[15] Mitochondrial and cytosolic fractions were prepared with digitonin-nagarse treatment. Protein concentrations were determined using a protein assay DC system (Bio-Rad, Richmond, CA, USA). Cell lysates (15 μg protein per lane) were fractionated in 12.5% SDS-polyacrylamide gels prior to transfer to the membranes (Immobilon-P membranes, Millipore, Bedford, MA, USA) using a standard protocol.

Antibody binding was detected by using an enhanced chemiluminescence kit for Western blotting detection with hyper-electrochemiluminescence film (Amersham, Buckinghamshire, UK). Blots were stained with Coomassie brilliant blue to confirm that there were equal amounts of protein extract on each lane. The following antibodies were used in this study: anti-caspase 3, -cytochrome *c* (PharMingen, San Diego, CA, USA), -Bcl-2, -BAX, -Bcl-X_L, -$p21^{CIP1/WAF1}$, -$p27^{KIP1}$, β-actin, -RARα, -Mcl-1, -survivin (Santa Cruz Biotech, Santa Cruz, CA), -cleaved PARP (Cell Signalling Technology, Inc., Beverly, MA, USA), and –Smac/DIABLO (MBL, Nagoya, Japan).

Animal model and experimental design

We have established the first human ATRA-resistant APL model in an NOD/SCID mice system using UF-1 cells.[16] Briefly, mice were pretreated with 3 Gy of total body irradiation, which is a sublethal dose that was expected to enhance the acceptance of xenografts. Subsequently, UF-1 cells (1×10^7 cells) in their logarith-

mic growth phase were inoculated subcutaneously into NOD/SCID mice (Jackson Laboratory, Bar Harbor, ME, USA). Inoculated UF-1 cells formed subcutaneous tumors at the injection site, and cells grew rapidly. Forty days after implantation of the cells, mice with the transplanted cells were randomly assigned to receive water (n=5) or 10 mM EGCG (n=5) as the sole drinking fluid administered daily for 12 days. After 12 days of treatment, mice were sacrificed and dissected to measure tumor weights. When the mice showed severe wasting or when observations were finished, they were sacrificed according to the UKCCCR guidelines, and the day of sacrifice was recorded.[17] Tumors were removed, fixed in 4% paraformaldehyde, and embedded in paraffin. Sections through the tumor were cut by a cryostat, and were mounted on glass slides for histological staining with hematoxylin and eosin. Mitotic cells in the same fields were counted in sections from both control and EGCG-treated animals, and expressed as the number of mitoses per field.

Statistical analysis

Tumor weights and the number of mitotic cells are expressed as mean ± SD. Differences in both parameters were analyzed for significance by Student's *t* test. $p<0.05$ was considered as statistically significant.

Results

Catechin inhibited cellular proliferation of various leukemic cells

We first examined whether the green tea polyphenols and the polyphenolic epicatechin derivatives induced inhibition of the growth of leukemic cells, including NB4, UF-1, HL-60, K562, and U937 cells. The structurally related catechins, i.e., EC, ECG, EGC and EGCG, inhibited the growth of leukemic cells. However, EGCG was the most potent inhibitor among the 4 derivatives (Figure 1). We thus used EGCG for the series of experiments. Treatment with EGCG for 24 h induced a marked inhibition of UF-1 cell growth and, to a lesser but significant extent, led to an inhibition of cellular growth in all other myeloid leukemic cells (Figure 2A). Among the cells tested, UF-1 cells were the most sensitive to EGCG with an IC50 of 50 μM (Figure 2A). Therefore, we used UF-1 cells for the further experiments.

EGCG induced G1 cell cycle arrest and subsequent apoptosis

The effects of EGCG on cell cycle progression were investigated using UF-1 cells. The cells were treated with 100 μM EGCG for 24 h and analyzed for cell cycle distribution by means of flow cytometry. Culture with EGCG increased the population of cells in the G1 phase from 69.9% to 91.0%, with a reduction of cells in the S phase from 27.7% to 7.5% (Figure 2B). In addition, a strong induction of apoptosis was shown by the appearance of a haplodiploid DNA peak with sub-G1 DNA contents at 24 h after treatment (Figure 2B). These results indicate that EGCG led to cell cycle arrest at the G1 phase followed by apoptosis. We thus confirmed the induction of apoptosis by EGCG by means of DNA ladder formation and annexin V/PI staining. Interestingly, DNA ladder formation was confirmed at a time point as early as 3 h by electrophoresis of genomic DNA extracted from UF-1 cells treated with 100 μM EGCG (Figure 2C). Consistent with these results, the numbers of annexin V-positive cells increased after incubation with EGCG for 3 h (Figure 2D), thus indicating that EGCG rapidly induced apoptosis in UF-1 and NB4 cells.

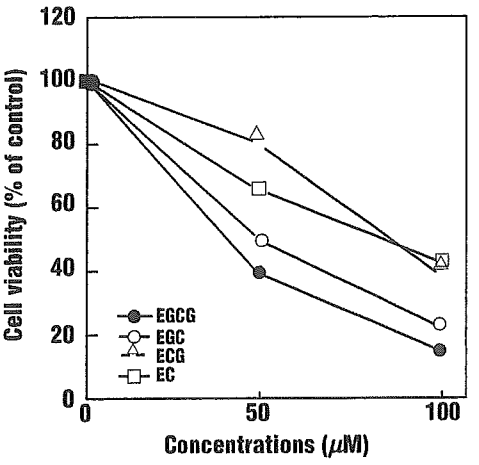

Figure 1. Effect of catechin derivatives on UF-1 cells. UF-1 cells were treated for 24 hours with the indicated dose of the major green tea polyphenols: (-)-epicatechin (EC), (-)-epicatechin-3-gallate (ECG), (-)-epigallocatechin (EGC), and (-)-epigallocatechin-3-gallate (EGCG). Cell viability was assessed by trypan blue dye exclusion. EGCG is the most potent inhibitor of leukemic cell growth.

Effects of EGCG on caspase-3 activity

To address the apoptotic pathway in EGCG-treated UF-1 cells, we next examined the activation of caspase-3 by Western blot analysis using antibody that recognizes both active and inactive forms of caspase-3. The 32-kDa procaspase-3 was cleaved into active forms (17kDa) after just 1 h of exposure to EGCG (100 μM) (Figure 3A). In addition, significant PARP cleavage was detected by 6 h of treatment with EGCG (Figure 3A). Furthermore, to elucidate the functional role of caspases in EGCG-induced apoptosis, experiments were performed with a series of caspase inhibitors. UF-1 cells were treated with 100 μM EGCG for 24 h, either alone or in combination with Z-VAD-FMK (pan caspase inhibitor), DEVD-CHO (caspase-3-specific inhibitor),

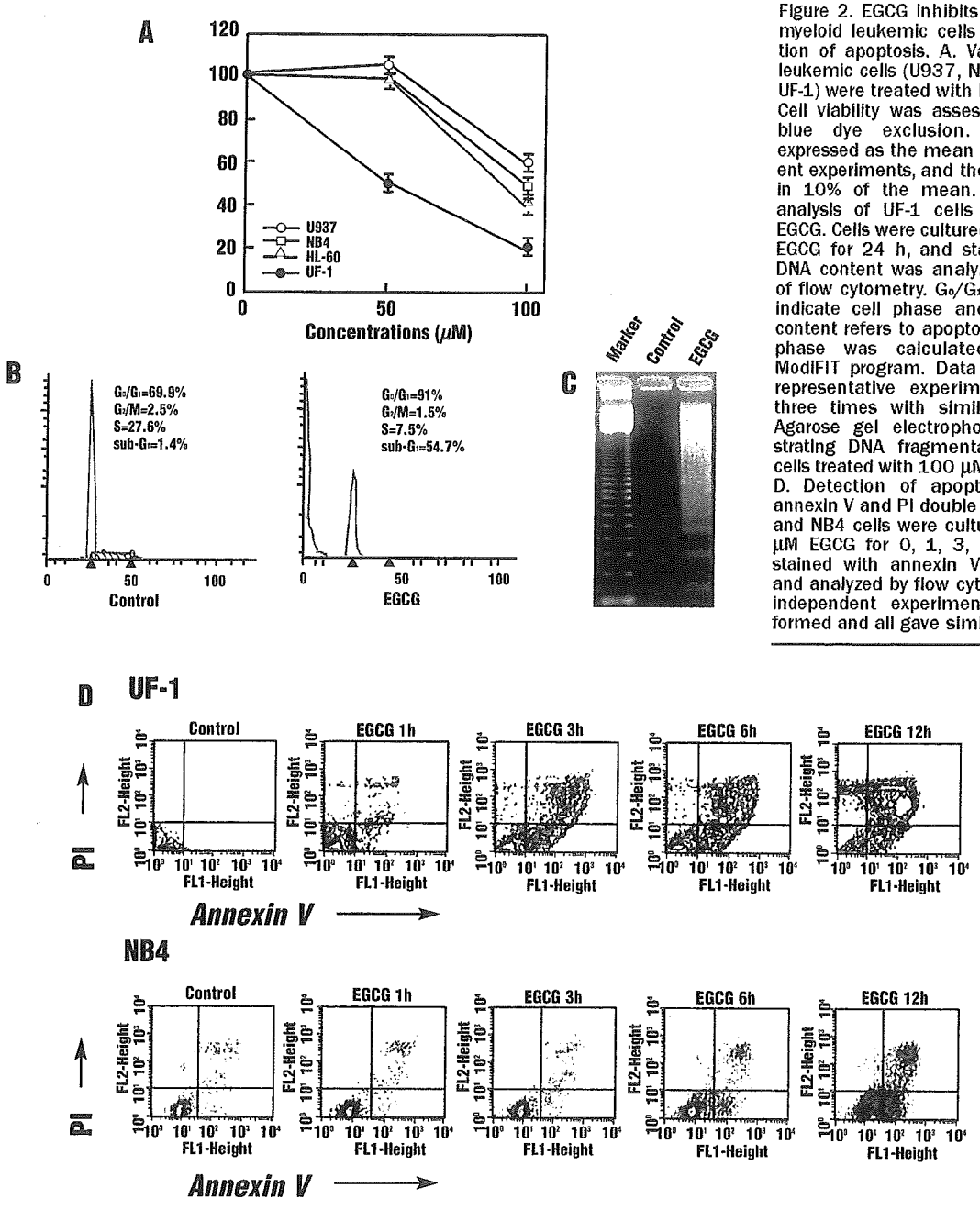

Figure 2. EGCG inhibits the growth of myeloid leukemic cells via the induction of apoptosis. A. Various myeloid leukemic cells (U937, NB4, HL-60 and UF-1) were treated with EGCG for 24 h. Cell viability was assessed by trypan blue dye exclusion. Results are expressed as the mean of three different experiments, and the SD was within 10% of the mean. B. Cell cycle analysis of UF-1 cells cultured with EGCG. Cells were cultured with 100 μM EGCG for 24 h, and stained with PI. DNA content was analyzed by means of flow cytometry. G_0/G_1, G_2/M, and S indicate cell phase and sub-G_1 DNA content refers to apoptotic cells. Each phase was calculated using the ModiFIT program. Data shown are a representative experiment repeated three times with similar results. C. Agarose gel electrophoresis demonstrating DNA fragmentation in UF-1 cells treated with 100 μM EGCG for 3h. D. Detection of apoptotic cells by annexin V and PI double staining. UF-1 and NB4 cells were cultured with 100 μM EGCG for 0, 1, 3, 6, and 12 h, stained with annexin V-FITC and PI, and analyzed by flow cytometry. Three independent experiments were performed and all gave similar results.

Z-IETD-FMK (caspase-8-specific inhibitor), or LEHD-CHO (caspase-9-specific inhibitor). EGCG-induced apoptosis was completely blocked by treatment with Z-VAD-FMK, DEVD-CHO, and LEHD-CHO, but not caspase-8-specific inhibitor, Z-IETD-FMK (Figure 3C). These results suggest that EGCG-induced apoptosis is associated with the activation of caspase-3 and -9, but not of caspase-8.

Expression of apoptosis-associated proteins

The expression of Bax protein was increased in a time-dependent manner by treatment with EGCG in UF-1 cells (Figure 4A). In contrast, EGCG did not modulate the levels of anti-apoptotic Bcl-2 and Bcl-X_L proteins in UF-1 cells. However, Bcl-2 family Mcl-1 and survivin were down-regulated after 6 h of EGCG treatment (Figure 4A). Expression of cdk inhibitors ($p21^{CIP1/WAF1}$ and $p27^{KIP1}$) was rapidly increased after 1 h exposure of EGCG in UF-1 cells (Figure 4B). UF-1 is a cell line from a patient with APL who had the chromosomal abnormality t(15;17), resulting in a *PML/RARA* fusion gene; this chimeric gene and its product may play important roles in leukemogenesis and development of this specific type of leukemia.[18] Therefore, we

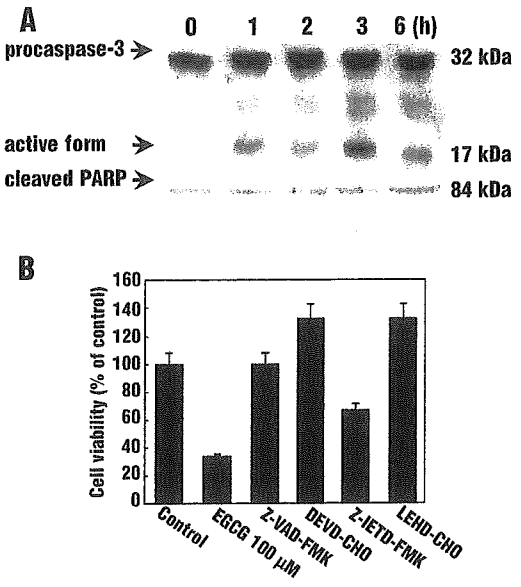

Figure 3. Effects of EGCG on caspase activation. A. Western blot analysis of caspase-3 and cleaved PARP. Total cellular proteins (15 μg per each lane) were separated on 12.5% SDS- polyacrylamide gels and transferred to the membrane. Protein levels of caspase-3 were detected by Western blot analysis using antibody against caspase-3. Treatment with EGCG (100 μM) induced processing of caspase-3 (32 kDa), indicated by the appearance of a 17 kDa cleaved active form. The anti-cleaved PARP antibody recognized cleaved PARP (84 kDa) in EGCG-treated UF-1 cells. Coomassie brilliant blue stain was used to confirm that each lane contained equal amounts of protein. B. Effects of caspase inhibitors on EGCG-treated UF-1 cells. Inhibition of EGCG-induced apoptosis of UF-1 cells was estimated in a co-culture with a series of caspase inhibitors. Cells were preincubated with each caspase inhibitor for 2 h prior to addition of 100 μM EGCG. Results are expressed as the mean ± SD of three different experiments. Z-VAD-FMK, pan caspase inhibitor; DEVD-CHO, caspase-3 inhibitor; Z-IETD-FMK, caspase-8 inhibitor; and LEHD-CHO, caspase-9 inhibitor.

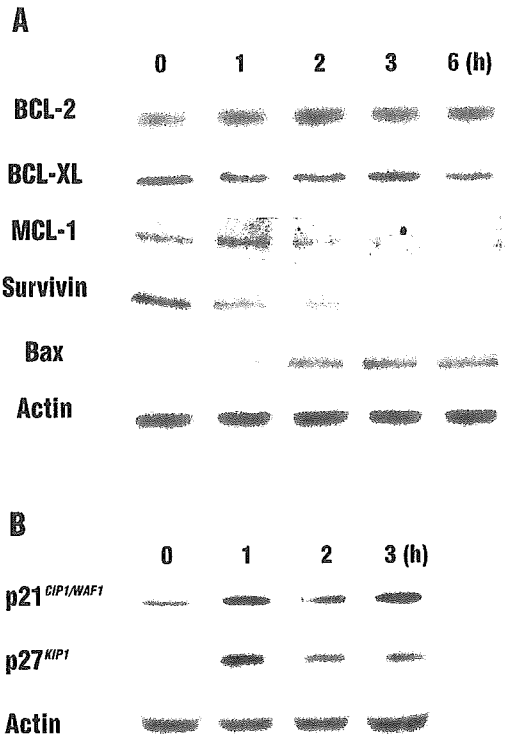

Figure 4. Expressions of the apoptosis-associated proteins and CDK inhibitors. A. UF-1 cells were treated with 100 μM EGCG for the indicated time. Cell lysates (15 μg per each lane) were fractionated on 12.5% SDS-polyacrylamide gels and analyzed by Western blotting with antibodies against Bcl-2, Bcl-Xʟ, MCl-1, survivin, Bax and β-actin proteins. B. The protein level of CDK inhibitors ($p21^{CIP1/WAF1}$, $p27^{KIP1}$) was detected by Western blotting. Re-blotting with β-actin staining demonstrated that equal amounts of protein were present in each lane.

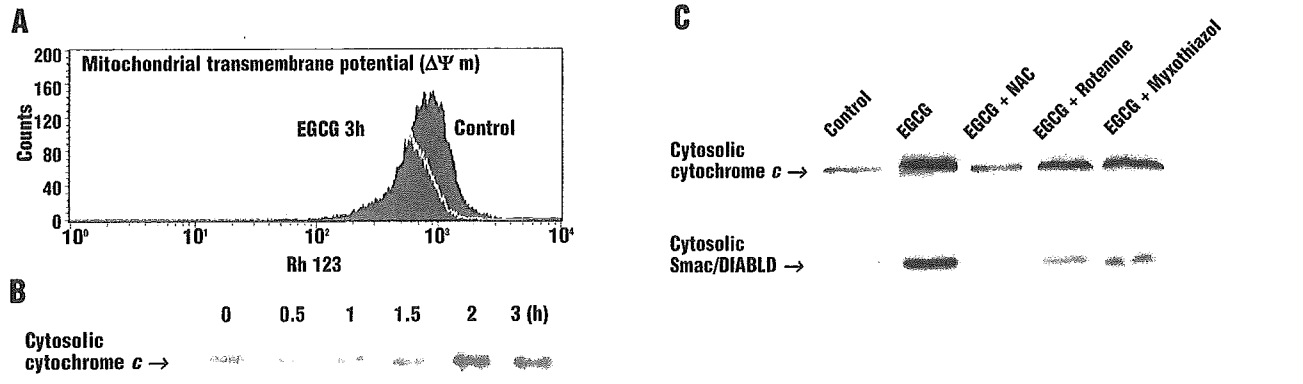

Figure 5. EGCG-induced apoptosis occurred via the mitochondrial pathway. A. Flow cytometric analysis of mitochindrial ΔΨm, as estimated by rhodamine 123 intensity. UF-1 cells were cultured with 100 μM EGCG for 3 hours, and rhodamine 123 fluorescence was analyzed by flow cytometry. B. Western blot analysis of cytochrome c in EGCG-treated UF-1 cells. Cells were incubated with 100 μM EGCG for the indicated time. The arrow indicates the expression of cytosolic cytochrome *c*. C. Effects of antioxidant and MRC inhibitors on the release of cytochrome *c* and Smac/DIABLO from the mitochondria to the cytosol during EGCG-induced apoptosis in UF-1 cells. UF-1 cells were pre-treated with NAC (10 mM), rotenone (1 μM), myxothiazol (100 nM) for 1 h, followed by the treatment of 100 μM EGCG for 3 h. The release of cytochrome c and Smac/DIABLO was analyzed by Western blotting.

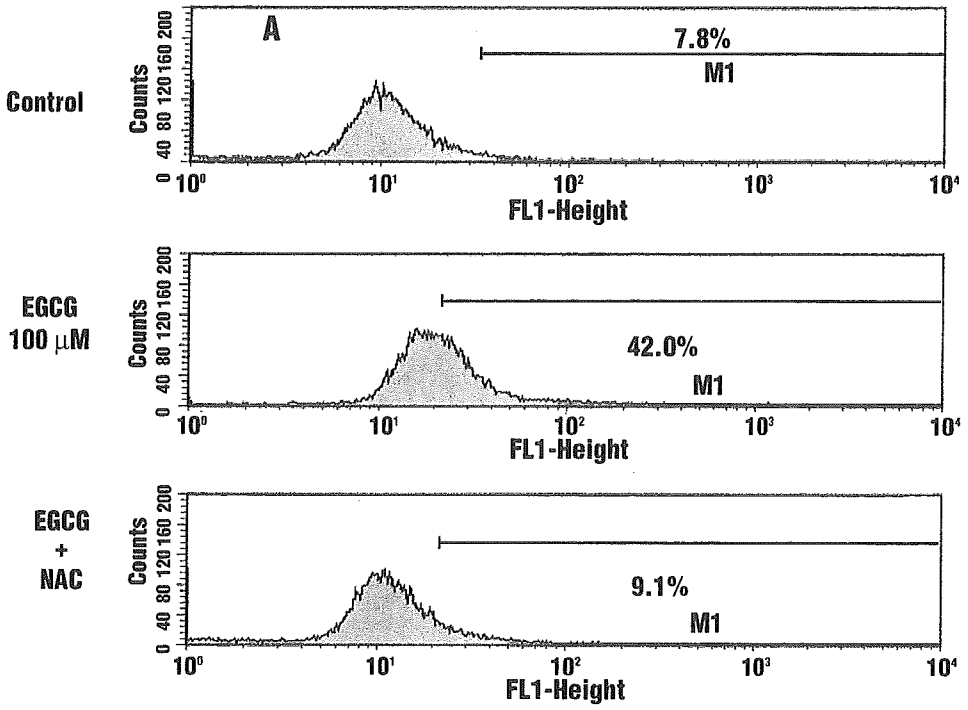

Figure 6. ROS generation by EGCG in UF-1 cells. To determine the intracellular concentration of ROS, UF-1 cells were cultured with DHE, and the fluorescence was measured by flow cytometry. DHE-derived fluorescence in untreated UF-1 cells and in cultures treated for 3 h with 100 μM EGCG is shown at the top and in the lower panel, respectively.

analyzed the effect of EGCG on this disease-specific chimeric protein. EGCG did not induce degradation of the PML/RARα chimeric protein (*data not shown*), suggesting that EGCG-induced apoptosis in UF-1 cells is not involved in the *PML/RARA* signaling pathway.

EGCG-induced death signaling is mediated through the mitochondrial pathway

Mitochondrial changes, including permeability transition pore opening and the collapse of $\Delta\psi_m$, result in the release of cytochrome c into the cytosol, which subsequently causes apoptosis by the activation of caspases.[19] After treatment with 100 μM EGCG for 3 h, low Rh123 staining in UF-1 cells indicated an increase in the loss of $\Delta\psi_m$ (Figure 5A). The loss of $\Delta\psi_m$ appeared in parallel with the activation of caspase-3 and -9, as well as with apoptosis. In addition, EGCG induced a substantial release of cytochrome c from the mitochondria into the cytosol in a time-dependent manner in UF-1 cells (Figure 5B). These results suggest that mitochondrial dysfunction causes the release of cytochrome *c* into the cytosol; caspase-9 and -3 were then activated, thereby propagating the death signal. The major sources of ROS are components of the mitochondrial respiratory chain (MRC). We also examined the role of the MRC components in EGCG-induced apoptosis in UF-1 cells by using MRC inhibitors, rotenone and myxothiazol. Antioxidant, NAC, completely inhibited the release of cytochtome c and Smac/DIABLO from the mitochondria into the cytosol, but MRC inhibitors caused partial inhibition (Figure 5C).

ROS production triggers EGCG-induced apoptosis

Several investigators have reported that EGCG-induced apoptosis is often associated with the generation of ROS.[6,20] We therefore analyzed the production of intracellular ROS in control and EGCG-treated cells. Treatment of UF-1 cells with 100 μM EGCG for 3 h caused dramatic oxidation of DHE to ethidium, and resulted in the induction of intracellular ROS (Figure 6A). Furthermore, treatment of UF-1 cells with a thiol antioxidant, NAC, an excellent supplier of glutathione (GSH), completely blocked generation of intracellular ROS and EGCG- induced apoptosis in UF-1 cells (Figure 6A and *data not shown*). Our data indicate that the modulation of molecules involved in the redox system, particularly that of the GSH, may determine the sensitivity of leukemia cells to EGCG. Furthermore, we examined the effect of EGCG on induction of apoptosis and ROS production in fresh leukemia cells from 6 patients with AML. These results were consistent with the results obtained from the previously mentioned cell lines, i.e., sensitivity to EGCG-induced apoptosis was

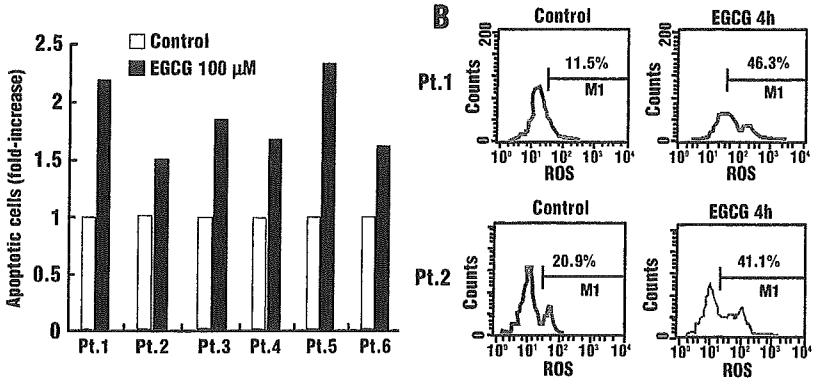

Figure 7. Effects of EGCG on fresh leukemic samples from patients with AML. Leukemic cells were separated by the Lymphoprep sedimentation procedure and subsequently cultured with 100 μM EGCG for 4 h. A. Apoptosis was evaluated by annexin V and PI double staining and showed the fold-increase of apoptotic cells in each case. B. Intracellular levels of ROS were measured by flow cytometry in representative EGCG-sensitive (Pt 1) and -less sensitive (Pt 2) cases. EGCG-sensitive leukemic cells are defined as those in which the increase of ROS production with treatment of EGCG is more than two-fold that in control cells.

observed in fresh leukemia cells from patients, and similarly increased production of intracellular ROS was also observed (Figure 7A and B). ROS production was 4.0 and 1.9-fold increased in EGCG-sensitive and -less sensitive fresh myeloid leukemic cells from the patients (patients 1 and 2, respectively) (Figure 7B).

EGCG induces apoptosis in vivo

Our *in vitro* data prompted us to examine whether the effects of EGCG are equally valid *in vivo*. After 40 days of implantation of UF-1 cells into NOD/SCID mice, water, used as a control (n=5), or 10 mM EGCG (n=5) treatment were administered orally as the sole drinking fluid ingested daily for 12 days. We found that tumor weight was significantly lower in the mice that were given EGCG compared to in the mice treated with water as a control ($p<0.05$, mean weight: 1.52g in the EGCG-treated group vs. 2.20g in the control group) (Figure 8A). During the treatment, the EGCG-treated mice appeared healthy and continued to eat. In addition, pathologic analysis at autopsy revealed no EGCG-induced tissue changes in any of the organs (*data not shown*). These results suggest that EGCG had no toxic effects on mice during the treatment. Tumor cell proliferation was evaluated by counting the number of mitoses. Comparing the number of mitoses by hematoxylin and eosin staining in the same fields, a significantly lower number was observed in the EGCG group ($p<0.001$, Figure 8B), suggesting that cell proliferation was more inhibited in the EGCG-treated mice than in the control mice.

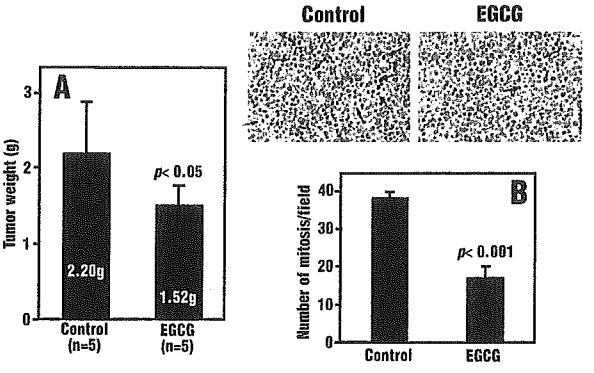

Figure 8. EGCG-mediated apoptosis of leukemic cells *in vivo* using an NOD/SCID mice model. A. UF-1 cells (1×10^7 cells) were inoculated subcutaneously into NOD/SCID mice. Forty days after transplantation, water (control) or 10 mM EOGCG was given as the sole drinking fluid daily for 12 days. After 12 days of treatment, mice were sacrificed and tumor weights were measured. Values shown are mean ± SD (*bars*). B. The tumor sections were fixed and stained with hematoxylin and eosin. The number of mitosis in the same fields was counted in both control and EGCG-treated tumor sections. Arrows indicate cells with mitoses. Values shown are mean ± SD (*bars*). Original magnification, × 100.

Discussion

Extensive *in vitro* cell culture studies, as well as *in vivo* studies in animal models, have verified the cancer preventive effects of green tea, and specifically, of its individual polyphenols.[21] Epidemiological studies, though inconclusive, have suggested that green tea may reduce the risks associated with many cancers including bladder, prostate, esophageal and gastric carcinomas.[2-6] Green tea extracts, especially its major polyphenolic component EGCG, are capable of inhibiting the growth of a variety of mouse and human cancer cells via the induction of *in vitro* apoptosis.[1,22,23] However, the precise mechanism of EGCG-induced apoptosis remains to be elucidated. In this study, we demonstrated that one green tea component in particular, EGCG, suppressed the cellular growth of various fresh leukemic cells and myeloid leukemia cell lines, especially promyelocytic UF-1 cells. The observed growth inhibition of leukemic cells was due to the induction of apoptosis. Mitochondria play an essential role in death signal transduction such that permeability tran-

sition pore opening and collapse of the $\Delta\psi_m$ resulted in the rapid release of caspase activators such as cytochrome *c* into the cytoplasm.[24] We demonstrated that the loss of the $\Delta\psi_m$ increased within 3 h of treatment, a time frame parallel to that of induced apoptosis. Furthermore, caspase-3 was activated by EGCG, and caspase-3 and caspase-9 inhibitors suppressed the apoptotic effects of EGCG. Taken together, these results suggest that EGCG-induced apoptosis in leukemic cells is associated with the loss of $\Delta\psi_m$ and with the activation of caspases, probably via the cytochrome *c*/Apaf-1/caspase-9 pathway. We further demonstrated that EGCG had no influence on the expression of Bcl-2 and Bcl-X_L, but it up-regulated the levels of Bax protein, and down-regulated the levels of Mcl-1 and survivin in UF-1 cells in a time-dependent manner. We detected that EGCG-induced apoptosis in UF-1 cells and in certain fresh leukemia samples was associated with an increase in the levels of intracellular ROS. It has been suggested that the generation of ROS is a common mechanism in one of the representative pathways of apoptosis.[20] Oxidants are capable of depleting GSH and damaging the cellular antioxidant defense system, and can directly induce apoptosis.[25-27] On the other hand, antioxidants such as NAC can inhibit apoptosis. Interestingly, a recent study using cDNA microarrays has identified that superoxide dismutases (SOD) are target molecules of estrogen-induced apoptosis in leukemic cells, and inhibition of SOD causes an accumulation of ROS and leads to the release of cytochrome *c* from the mitochondria.[28] Although EGCG is generally well-known as an antioxidant, it can also behave as a pro-oxidant under certain conditions.[6,29] Therefore, we hypothesized that EGCG-induced apoptosis is also related to the GSH redox system, in a manner similar to the As_2O_3-induced apoptosis in APL cells.[30,31] An antioxidant, NAC, increased intracellular GSH contents and completely blocked EGCG-induced apoptosis. In contrast, MRC inhibitors, rotenone and myxothiazol, partially blocked EGCG-induced cytochrome *c* and Smac/DIABLO release from the mitochondria to the cytosol, suggesting that MRC is required for the induction of apoptosis of the leukemic cells via mitochondrial ROS production by treatment with EGCG. EGCG was able to induce G1 cell cycle arrest in the leukemic cells. The loss of cell cycle checkpoints in cancer cells confers a growth advantage.[32-34] Therefore, EGCG suppresses cell growth by imposing cell cycle checkpoints in leukemic cells. To clarify the mechanisms of EGCG effects on the cell cycle, we examined the expression of cell cycle-associated proteins, including CDK, CDK inhibitors and various cyclins by Western blot analysis. Expression of $p21^{CIP1/WAF1}$ and $p27^{KIP1}$ increased in a time-dependent manner, whereas the expression of cyclin D1, cyclin E, CDK2, and CDK4 were not altered by EGCG (*data not shown*). Up-regulation of $p21^{CIP1/WAF1}$ and $p27^{KIP1}$ may thus play a pivotal role in inducing cell cycle arrest and apoptosis in EGCG-treated UF-1 cells. Recent studies have also indicated that green tea is an effective inhibitor of angiogenesis *in vivo*.[35,36]

Catechin, a component of green tea, is a natural compound, and it appears to be safer than current chemotherapeutic drugs. Since we could not observe any organ damage *in vivo*, catechin might be developed as a new potent anti-cancer agent for the management of hematologic malignancies. In particular, it might be useful in older patients or in immunocompromised patients because of its safety and lack of known toxicity. Since green tea extracts have already entered phase I trials in patients with solid tumors in the USA,[37] it would be useful to design similar clinical trials with leukemic patients to evaluate its anti-leukemic effects. In conclusion, this component of green tea may have potential as a novel therapeutic agent to replace or augument the more cytotoxic agents currently used to treat the patients with leukemia.

TN: performed the research and wrote the first version of the paper; KI: performed FACS analysis; YM, KK: planned in vivo experiments and managed patients; TY, NH: performed in vivo experiments and histological analyses; AI: collected patients' samples and analyzed clinical data; MK: designed the whole research and wrote the final version of this manuscript. The authors declare that they have no potential conflict of interest.

This work was supported in part by grants from the Ministry of Education, Culture, Sports, Science, and Technology of Japan; the Keio University Medical Science Fund from Keio University; and the Chamber of Commerce in Green Tea of Kyoto Prefecture in Japan.

Manuscript received May 11, 2004. Accepted January 7, 2005

References

1. Yang CS, Wang ZY. Tea and cancer (review). J Natl Cancer Inst 1993;85: 1038-49.
2. Asano Y, Okamura S, Ogo T, Eto T, Otsuka T, Niho Y. Effect of (-)-epigallocatechin gallate on leukemic blast cells from patients with acute myeloblastic leukemia. Life Sci 1997; 60:135-42.
3. Lea MA, Xiao Q, Sadhukhan AK, Cottle S, Wang ZY, Yang CS. Inhibitory effects of tea extracts and (–)-epigallocatechin gallate on DNA synthesis and proliferation of hepatoma and erythroleukemia cells. Cancer Lett 1996;68:231-6.
4. Valcic S, Timmermann BN, Alberts DS, Wachter GA, Kurtzsch M, Wymer J, et al. Inhibitory effect of six green tea catechins and caffeine on the growth of four selected human tumor cell lines. Anticancer Drugs 1996;7:461-8.
5. Liao S, Umekita Y, Guo J, Kokontis JM, Hiipakka RA. Growth inhibition and regression of human prostate and breast tumors in athymic mice by epigallocatechin gallate. Cancer Lett 1995;25:239-43.
6. Islam S, Islam N, Kermode T, Johnstone B, Mukhtar H, Moskowitz RW, et al. Involvement of caspase-3 in epigallocatechin-3-gallate-mediated apoptosis of human chondrosarcoma cells. Biochem Biophys Res Commun 2000;270:793-7.
7. Ahmad N, Feyes DK, Nieminen AL, Agarwal R, Mukhtar H. Green tea constituent epigallocatechin-3-gallate and induction of apoptosis and cell cycle arrest in human carcinoma cells. J Natl Cancer Inst 1997;89:1881-6.
8. Lepley DM, Li B, Birt DF, Pelling JC. The chemopreventive flavonoid api-